

Oct 15, 2020

Dear Editor,

Thank you very much for your editing work on our paper entitled “Revisiting the Relationship between Atlantic Dust and Tropical Cyclone Activity using Aerosol Optical Depth Reanalyses: 2003–2018”. Thank you also for your suggestion of emphasizing the key findings of the paper in the abstract and conclusions, which would make the key findings standing out more. In response to your suggestion, we have added one concluding sentence in the abstract and a similar concluding sentence in the last paragraph of the conclusions section. We hope you find this technical correction is satisfactory. The concluding sentence in the abstract reads

“Overall, DAOD in both the tropical Atlantic and Caribbean is negatively correlated with Atlantic hurricane frequency and intensity, with stronger correlations in the Caribbean than farther east in the tropical North Atlantic.”

In addition, we have revised the reference format in the paper following ACP’s reference guidance in response to the advice from your editorial team. The manuscript with marked up changes are attached below.

Sincerely,

Peng

Peng Xian, PhD
Atmospheric Properties and Effects
Naval Research Laboratory
Marine Meteorology Division
7 Grace Hopper Avenue, Stop 2
Monterey, California 93940
831-656-4803
FAX 831-656-4769
peng.xian@nrlmry.navy.mil

1 **Revisiting the Relationship between Atlantic Dust and Tropical Cyclone**
2 **Activity using Aerosol Optical Depth Reanalyses: 2003-2018**

3
4 Peng Xian^{1a}, Philip J. Klotzbach^{2a}, Jason P. Dunion³, Matthew A. Janiga¹, Jeffrey S. Reid¹, Peter
5 R. Colarco⁴ and Zak Kipling⁵

6
7 ¹Naval Research Laboratory, Monterey, CA, USA.

8 ²Department of Atmospheric Science, Colorado State University, Fort Collins, CO, USA.

9 ³University of Miami/RSMAS/CIMAS – NOAA/AOML/Hurricane Research Division, Miami,
10 FL, USA.

11 ⁴NASA Goddard Space Flight Center, Greenbelt, MD, USA.

12 ⁵European Centre for Medium-Range Weather Forecasts, Reading, UK.

13
14 ^a Peng Xian and Philip J. Klotzbach are joint-lead coauthors.

15 Correspondence: Peng Xian (peng.xian@nrlmry.navy.mil)

35 **Abstract**

36 Previous studies have noted a relationship between African dust and Atlantic tropical cyclone
37 (TC) activity. However, due to the limitations of past dust analyses, the strength of this
38 relationship remains uncertain. The emergence of aerosol reanalyses, including the Navy Aerosol
39 Analysis and Prediction System (NAAPS) Aerosol Optical Depth (AOD) reanalysis, NASA
40 Modern-Era Retrospective analysis for Research and Applications, Version-2 (MERRA-2) and
41 ECMWF Copernicus Atmosphere Monitoring Service reanalysis (CAMSR) enable an
42 investigation of the relationship between African dust and TC activity over the tropical Atlantic
43 and Caribbean in a consistent temporal and spatial manner for 2003-2018. Although June-July-
44 August (JJA) 550 nm dust AOD (DAOD) from all three reanalysis products correlate
45 significantly over the tropical Atlantic and Caribbean, the difference in DAOD magnitude
46 between products can be as large as 60% over the Caribbean and 20% over the tropical North
47 Atlantic. Based on the three individual reanalyses, we have created an aerosol multi-reanalysis-
48 consensus (MRC). The MRC presents overall better root mean square error over the tropical
49 Atlantic and Caribbean compared to individual reanalyses when verified with ground-based
50 AEROSOL ROBOTIC NETWORK (AERONET) AOD measurements. Each of the three individual
51 reanalyses and the MRC have significant negative correlations between JJA Caribbean DAOD
52 and seasonal Atlantic Accumulated Cyclone Energy (ACE), while the correlation between JJA
53 tropical North Atlantic DAOD and seasonal ACE is weaker. Possible reasons for this regional
54 difference are provided. A composite analysis of three high versus three low JJA Caribbean
55 DAOD years reveals large differences in overall Atlantic TC activity. We also show that JJA
56 Caribbean DAOD is significantly correlated with large-scale fields associated with variability in
57 interannual Atlantic TC activity including zonal wind shear, mid-level moisture and SST, as well
58 as ENSO and the Atlantic Meridional Mode (AMM), implying confounding effects of these
59 factors on the dust-TC relationship. We find that seasonal Atlantic DAOD and the AMM, the
60 leading mode of coupled Atlantic variability, are inversely related and intertwined in the dust-TC
61 relationship. Overall, DAOD in both the tropical Atlantic and Caribbean is negatively correlated
62 with Atlantic hurricane frequency and intensity, with stronger correlations in the Caribbean than
63 farther east in the tropical North Atlantic.

64

65 1. Introduction

66 Saharan dust particles can affect weather and climate through both direct and indirect radiative
67 and cloud processes, notably in association with boreal summer Saharan Air Layer (SAL)
68 outbreaks. The SAL is a layer of hot and dry air that forms over continental West Africa and is
69 then advected over the low-level moist marine boundary layer of the tropical Atlantic (Carlson
70 [and](#) Prospero, 1972). The SAL is often associated with the African Easterly Jet (AEJ) that can
71 enhance vertical wind shear. Despite numerous observational and modeling studies that have
72 examined the relationships between these aspects of the SAL and Atlantic TC activity, there are
73 conflicting findings as to whether dust acts to generally inhibit or enhance tropical cyclogenesis
74 and intensification. Some studies suggest negative impacts of the SAL's dust-laden dry air and
75 the AEJ on TC activity (e.g., Dunion and Velden 2004; Lau and Kim 2007; Jones et al. 2007;
76 Sun et al. 2008; Pratt and Evans 2008) while others have focused exclusively on the dust
77 particles themselves and have found a negative influence on TCs (e.g., Evan et al. 2006a;
78 Rosenfield et al. 2007; Strong et al. 2018; Reed et al. 2019). Other studies have suggested little
79 impact of the SAL on TCs (e.g., Braun 2010; Sippel et al. 2011; Braun et al. 2013), while others
80 have posited a positive impact of dust on TCs through cloud-microphysical processes (e.g.,
81 Jenkins et al. 2008). Finally, others have suggested that there are contrasting influences through
82 different mechanisms and for different TCs (Karyampudi and Pierce, 2002; Bretl et al. 2015; Pan
83 et al., 2018), highlighting the complexity of the dust-TC interaction.

84 African dust impacts the North Atlantic throughout the year, with its summer peak season (May-
85 August) overlapping and leading the peak of the Atlantic hurricane season (August-October;
86 Figure S1). As African dust outbreaks during the summer are often associated with the SAL,
87 airborne dust has often been used as an indicator for the SAL (Dunion [and](#) Velden, 2004;
88 Dunion, 2011; Tsamalis et al., 2013), although early season cases where the majority of the dust
89 existed in the marine boundary layer below the trade wind inversion instead of staying aloft were
90 also found (Reid et al., 2003). Saharan dust and the SAL are frequently observed throughout the
91 Caribbean and as far west as Central America and the North American continent during the
92 boreal summer (e.g., Prospero, 1999; Reid et al., 2003; Dunion [and](#) Velden 2004; Nowotnick
93 et al., 2011; Kuciauskas et al., 2018). Airborne dust associated with the SAL often extends to 5.5
94 km (500 hPa) off of western Africa, and becomes thinner as its top lowers and its base rises as it
95 is advected westward, shrinking to below 2 km in the Caribbean and in the Gulf of Mexico
96 (Tsamalis et al., 2013). In some strong SAL cases, however, the top of the dust layer can reach 6
97 km (Reid et al., 2003; Colarco et al., 2003). During their trans-Atlantic transport, dust aerosols
98 are from time to time observed to interact with TCs, as seen in satellite imagery (Figure 1).

99 African dust and its associated SAL has been hypothesized to impact TCs through a variety of
100 mechanisms. Through scattering and absorbing sunlight, dust reduces solar radiation reaching
101 the surface, thus cooling SSTs (e.g., Miller and Tegen, 1998; Lau and Kim 2007; Evan et al.,
102 2009). Lower SSTs provide TCs with less energy to initiate, develop, and maintain strength.
103 Through additional radiative heating of the dusty layer, mineral dust is also suggested to impact
104 the structure, location and energetics of the AEJ (Tompkins et al., 2005; Wilcox et al., 2010;
105 Reale et al., 2011) and African easterly wave (AEW) activity (Karyampudi and Carlson, 1988;
106 Reale et al., 2009; Nathan et al., 2017; Jones et al., 2004; Ma et al., 2012; Grogan et al., 2016,
107 2017; Bercos-Hickey et al., 2017), thus having implications for tropical cyclogenesis. From a
108 thermodynamic point of view, Dunion and Velden (2004) have proposed that the dust-carrying

109 SAL outbreaks could inhibit TC formation and development in the North Atlantic through three
110 primary mechanisms, including dry air intrusion into the storm, enhancement of the local vertical
111 wind shear associated with the enhanced AEJ, and stabilization of the environment due to
112 radiative heating of the dust layer above the marine boundary layer.

113 Dust particles can also act as cloud condensation nuclei (Twohy et al., 2009; Karydis et al.,
114 2011) and ice nuclei (DeMott et al., 2003; Sassen et al., 2003) and affect cloud microphysics,
115 weakening or strengthening convection depending on the environment (Khain, 2009). Focusing
116 specifically on TCs, there is not a consistent conclusion among studies on whether the
117 microphysical impacts of dust weaken or strengthen TCs (Jenkins et al., 2008; Rosenfeld et al.,
118 2007; Zhang et al., 2007, 2009; Herbener et al., 2014; Nowottnick et al., 2018).

119 While dust aerosols can affect TC formation and development through radiative and cloud-
120 microphysical impacts, TCs can in turn impact dust aerosol spatial distributions through wet
121 removal and dynamic flow (Herbener et al., 2016). AEWs, serving as seeding disturbances for
122 TCs (Landsea, 1993), are shown to contribute to dust emission and transport (e.g., Westphal et
123 al., 1987; Jones et al., 2003; Knippertz and Todd, 2010). Climate variability that affects TC
124 activity can also impact African dust emission and transport over the North Atlantic and
125 Caribbean. For example, ENSO was found to affect the emission and transport of African dust as
126 well (Prospero [and](#) Lamb, 2003; DeFlorio et al., 2016), especially during the boreal winter
127 (Prospero [and](#) Nees, 1986; Evan et al., 2006b).

128 How all of these factors interact in the complex climate system and to what extent they can
129 impact TC formation and intensification is still largely unknown. The goal of this study is to
130 explore how the integrated interactions manifest themselves in the relationship between Saharan
131 dust and Atlantic TC activity on seasonal to interannual time scales using state-of-the-art aerosol
132 reanalysis data. This serves as a first step towards further understanding the dust-TC relationship
133 and evaluating the relative importance of different mechanisms. Previous empirical studies on
134 the relationship between African dust and Atlantic TC activity are limited by uneven spatial and
135 temporal sampling by satellite and in situ-based observations. The emergence of several aerosol
136 reanalysis datasets, including the Navy Aerosol Analysis and Prediction System (NAAPS)
137 Aerosol Optical Depth (AOD) reanalysis (NAAPS-RA, Lynch et al., 2016), the Modern-Era
138 Retrospective analysis for Research and Applications, Version 2 (MERRA-2) aerosol reanalysis
139 (Randles et al., 2017) and the Copernicus Atmosphere Monitoring Service ReAnalysis
140 (CAMSRA) (Inness et al., 2019) allow us to investigate this relationship in a more consistent
141 manner over their joint time period to provide a degree of statistical robustness.

142 In section 2, an introduction to the aerosol and large-scale environmental data and the analysis
143 methods employed is provided. Section 3 presents the DAOD climatology, its interannual
144 variability over the Atlantic, and comparisons of the three aerosol reanalyses. This section also
145 evaluates correlations between DAOD and Atlantic TC activity, as well as the relationship
146 between DAOD and large-scale environmental conditions and climate modes. The sensitivity of
147 the results to the definition of the regions, the number of composite years used, and the definition
148 of dust seasons are provided in section 4. A discussion and conclusions are given in section 5.

149 **2. Data and Methods**

150 **2.1 Methods**

151 Regardless of the underlying mechanisms, as there are contradicting mechanisms proposed in
152 different studies, the goal of this study is to examine if there is a robust and statistically
153 significant relationship between African dust and Atlantic TC activity on seasonal to interannual
154 time scales. We also examine if there are confounding factors, for example, meteorological
155 conditions and climate modes that co-vary with dust and hence influence TC activity.

156 We use dust AOD (DAOD) to represent Atlantic dust levels. Three aerosol reanalysis products,
157 and their consensus DAOD are used in order to increase the fidelity of the analysis result, given
158 that multi-model-consensus typically has been shown to have better data quality in prior
159 assessments (Sessions et al., 2015; Xian et al., 2019). Various TC count indices and
160 Accumulated Cyclone Energy (ACE) (Bell et al. 2000), defined in the next section, are utilized
161 to represent TC activity.

162 The Atlantic Main Development Region (MDR) (e.g., Goldenberg et al., 2001), including the
163 Caribbean (10-20°N, 85-60°W) and the tropical North Atlantic (10-20°N, 60-20°W), are the
164 focus regions for this study (see also Figure 2 for a spatial representation of the two subregions).
165 Most previous studies of dust impacts on TC activity have focused on the tropical North Atlantic
166 or regions closer to the African continent (e.g., Karyampudi and Pierce, 2002; Bretl et al. 2015;
167 Pan et al., 2018) where DAOD is relatively high. However significant dust pulses can also be
168 transported into the Caribbean. We therefore expand our study area to explore the potential
169 impacts of high levels of dust in the Caribbean on Atlantic TC activity. This allows us to explore
170 regional differences in the dust-TC relationship. Statistical relationships between DAOD and TC
171 activity over the MDR are investigated using the three aerosol reanalyses and multi-reanalysis-
172 consensus (MRC). The results obtained herein also help us assess the potential of using DAOD
173 to aid in future Atlantic seasonal hurricane forecasts.

174 The correlations between variables of interest are based on the Pearson correlation coefficient.
175 Statistical significance is assessed at the 95% level using a two-tailed Student's t-test.
176 Correlations ≥ 0.51 are statistically significant given that a 16-year time period (e.g., 2003-
177 2018) is investigated here. For partial correlation analysis, partial correlations ≥ 0.55 are
178 statistically significant at the 95% level with 13 degrees of freedom. The criteria for statistical
179 significance with various degrees of freedom can also be obtained at:
180 <https://www.esrl.noaa.gov/psd/data/correlation/significance.html>.

181 **2.2 Aerosol data**

182 A combination of aerosol reanalyses are used to describe the aerosol environment over the
183 tropical North Atlantic and Caribbean. An aerosol multi-reanalysis-consensus (MRC) based on
184 three aerosol reanalysis products, including the NAAPS-RA (Lynch et al., 2016) from the US
185 Naval Research Laboratory, MERRA-2 (Randles et al., 2017) from NASA, and CAMSRA
186 (Inness et al., 2019) from ECMWF, are also generated and used. The analysis period is focused
187 on 2003-2018, when all three aerosol reanalyses are available and both Terra and Aqua Moderate
188 Resolution Imaging Spectroradiometer (MODIS) AOD retrievals were assimilated therein.

189 **2.2.1 NAAPS AOD reanalysis**

190 The NAAPS-RA product provides 550 nm speciated AOD at a global scale with $1^\circ \times 1^\circ$ degree
191 spatial and 6-hourly temporal resolution for the years 2003-2018 (Lynch et al., 2016). This

192 reanalysis uses a modified version of NAAPS and assimilates quality-controlled AOD retrievals
193 from MODIS on Terra and Aqua and the Multi-angle Imaging SpectroRadiometer (MISR) on
194 Terra (Zhang et al., 2006; Hyer et al., 2011; Shi et al., 2011). NAAPS characterizes
195 anthropogenic and biogenic fine aerosol species (ABF), dust, sea salt and biomass burning
196 smoke aerosols. The aerosol source functions were tuned regionally so that a best match between
197 the model coarse and fine mode AODs and the Aerosol Robotic Network (AERONET) AODs
198 can be obtained. Other model processes, e.g. deposition, were also tuned to minimize the AOD
199 difference between the model and quality-controlled satellite AOD retrievals. NOAA Climate
200 Prediction Center MORPHing (CMORPH) precipitation derived from satellite observations
201 (Joyce et al., 2004) is used to correct precipitation biases in the tropics for better AOD analyses
202 through wet deposition processes (Xian et al., 2009). The reanalysis captures the decadal AOD
203 trends detected using standalone satellite products in other studies (e.g., Hsu et al., 2012; Zhang
204 et al., 2017), demonstrating the quality of the reanalysis product for climate studies. The
205 NAAPS-RA data for May 2017 - November 2018 was generated by assimilating MODIS DA-
206 quality AOD only without MISR AOD assimilation because of the unavailability of MISR DA-
207 quality data at the time of this study. The impact of not including MISR is expected to be minor
208 as MISR provides only about 10% of the total assimilated AOD data. Additionally, differences
209 between monthly mean DA-quality AOD over the MDR region derived using both MODIS and
210 MISR versus using only MODIS were found to be negligible (not shown).

211 **2.2.2 MERRA-2 AOD reanalysis**

212 As part of the upgrade from the original MERRA reanalysis (Rienecker et al., 2011) based on the
213 Goddard Earth Observing System (GEOS) Earth system model, MERRA-2 now incorporates
214 assimilation of AOD from a variety of remote sensing sources, including AERONET, MODIS,
215 and MISR after 2000, and AVHRR before 2002. The aerosol module used for MERRA-2 is the
216 Goddard Chemistry, Aerosol, Radiation, and Transport model (GOCART; Chin et al. 2000;
217 Colarco et al., 2010), which provides simulations of dust, sea salt, black and organic carbon, and
218 sulfate aerosols, and is run radiatively coupled to the GEOS AGCM. A detailed description and
219 validation of the AOD reanalysis product can be found in Randles et al. (2017) and Buchard et
220 al. (2017). For the purpose of this study, monthly mean DAOD at 550 nm with 0.5° latitude and
221 0.625° longitude spatial resolution is used. MERRA-2's longer data record (1981-present)
222 would have made it an ideal candidate for a longer-period analysis of the relationship between
223 DAOD and TCs. However, the volcanic eruptions of El Chichon (1982) and Pinatubo (1991)
224 result in high AOD for several years following each event, and the particle property assumptions
225 in MERRA-2 do not properly apportion the assimilated AOD increments among the simulated
226 aerosol species. For the 2003-2018 time period, MERRA-2 AOD data has similar validation
227 statistics compared to NAAPS-RA and CAMSRA at the sites located off of the coast of West
228 Africa and the Caribbean, as shown in Table 1.

229 **2.2.3 CAMSRA AOD reanalysis**

230 Under the banner of the Copernicus Atmosphere Monitoring Service (CAMS), operated by
231 ECMWF on behalf of the European Commission, a new global reanalysis of atmospheric
232 composition has been produced: CAMSRA (Inness et al., 2019). This is the successor to the
233 MACC reanalysis (Inness et al., 2013) and CAMS interim reanalysis (Flemming et al., 2017)
234 produced previously at ECMWF. The dataset spans the period 2003–2018 and is being continued
235 for subsequent years. The model component is based on the same Integrated Forecasting System

236 (IFS) used at ECMWF for weather forecasting and meteorological reanalysis, but at a coarser
237 resolution and with additional modules activated for prognostic aerosol species (dust, sea salt,
238 organic matter, black carbon and sulphate) and trace gases. The impact of the aerosols (and
239 ozone) on radiation and thereby on meteorology is included in the model. For aerosol,
240 observations of total AOD at 550nm are assimilated from MODIS (Terra and Aqua) for the
241 whole period, and from the Advanced Along-Track Scanning Radiometer for 2003–2012, using a
242 4D variational data assimilation system with a 12-hour data assimilation window along with
243 meteorological and trace gas observations. The speciated AOD products used in this study are
244 available at a 3-hourly temporal resolution and a $\sim 0.7^\circ$ spatial resolution. Model development
245 has generally improved the speciation of aerosols compared with earlier reanalyses, and
246 evaluation against AERONET is largely consistent over the period of the reanalysis. There is a
247 known issue regarding a significant overestimation of sulfate near outgassing volcanoes;
248 however this is unlikely to have much relevance to the regions considered in this study.

249 **2.2.4 AOD multi-reanalysis-consensus (MRC)**

250 Based on the three aerosol reanalysis products described above, we made a MRC product
251 following the multi-model-ensemble method of the International Cooperative for Aerosol
252 Prediction (ICAP, Sessions et al., 2015; Xian et al., 2019). The MRC is a consensus mean of the
253 three individual reanalyses, with a $1^\circ \times 1^\circ$ degree spatial and monthly temporal resolution.
254 Speciated AODs and total AOD at 550nm for 2003-2018 are available. This new product is
255 validated with ground-based AERONET observations for African-dust-influenced regions,
256 including the western coast of North Africa and the Caribbean Sea. Validation results in terms of
257 RMSE for total and coarse-mode AODs are presented in Table 1. Similar to the ICAP multi-
258 model-ensemble evaluation result, the MRC is found to generally be the top performer among all
259 of the reanalyses for the study region.

260 **2.2.5 AEROSOL ROBOTIC NETWORK (AERONET) FINE AND COARSE MODE AOD**

261 AERONET is a ground-based global scale sun photometer network that includes instruments to
262 measure sun and sky radiance at wavelengths ranging from the near ultraviolet to the near
263 infrared during daytime hours. This network has been providing high-accuracy and high-quality
264 measurements of aerosol properties since the 1990s (Holben et al., 1998; Holben et al., 2001)
265 and is often used as the primary dataset for validating aerosol optical properties in satellite
266 retrievals and model simulations (e.g., Levy et al., 2010; Colarco et al., 2010; Kahn ~~and~~
267 Gaitley, 2015). Only cloud-screened, quality-assured version 3 Level 2 AERONET data are
268 utilized in this study (Giles et al., 2019). AERONET multiple wavelength measurements were
269 used to derive both fine and coarse mode AODs at 550 nm based on the Spectral Deconvolution
270 Method (SDA) of O'Neill et al. (2003). The SDA product was verified with in situ
271 measurements (Kaku et al., 2014) and was shown to be able to capture the full modal properties
272 of fine and coarse particles. Temporally, AERONET data are averaged into 6-hr bins centered at
273 the regular model output times of 0, 6, 12 and 18 UTC. Monthly mean AERONET AOD is
274 derived only when the total number of 6-hr AERONET data is greater than 18 to ensure temporal
275 representativeness.

276 **2.3 Tropical Cyclone data – HURDAT2**

277 Atlantic basin TC data were taken from the Atlantic hurricane database version 2 (HURDAT2;
278 Landsea [and](#) Franklin, 2013). This dataset contains six-hourly information (including position,
279 maximum sustained winds, and central pressure – where available) for every TC observed in the
280 Atlantic basin dating back to 1851.

281 **2.4 Atmospheric data - ERA-Interim Reanalysis**

282 The ERA-Interim Reanalysis (Dee et al., 2011) is a global atmospheric reanalysis produced by
283 the ECMWF that uses a 4-dimensional variational analysis with a 12-hour analysis window. The
284 spectral resolution of this data is approximately 80 km (T255) and is available on 60 vertical
285 levels from the surface to 0.1 hPa and is available from January 1979 – August 2019. We use
286 monthly mean large-scale fields, including vector wind, atmospheric temperature and relative
287 humidity data on several pressure levels.

288 **2.5 Oceanic data - NOAA OI SST**

289 The National Oceanic and Atmospheric Administration (NOAA) Optimum Interpolation (OI)
290 SST product (Reynolds et al., 2002) is utilized for SST calculations. NOAA OI SST v2 uses a
291 combination of in-situ data, satellite data, SSTs simulated by sea-ice cover, and bias adjustments
292 to arrive at its final estimate of SSTs. NOAA OI SST V2 data is available on a 1° x 1° grid from
293 November 1981-present.

294 **2.6 Climate indices**

295 The Oceanic Niño Index (ONI), defined to be a three-month average of the Niño 3.4 (5°S-5°N,
296 170-120°W) index (Barnston et al., 1997) based on centered 30-year periods which are updated
297 every five years, is utilized to represent the state of El Niño-Southern Oscillation (ENSO). This
298 index is also used by NOAA to identify ENSO events.

299 The SST component of the AMM (Kossin [and](#) Vimont, 2007) is investigated to assess the
300 relationship between DAOD and tropical Atlantic oceanic conditions. While the index is not
301 standardized, we have standardized it by its 1981-2010 average and standard deviation.

302 **2.7 Derived tropical cyclone indices**

303 The genesis potential index (GPI) was calculated using monthly-averaged ERA-Interim data
304 following Emanuel and Nolan (2004). The maximum potential intensity (MPI) was calculated
305 using monthly-averaged ERA-Interim temperature and moisture and NOAA OI SST following
306 Bister and Emanuel (2002).

307 **3. Results**

308 **3.1 Dust aerosol optical depth over the MDR (2003-2018)**

309 Figure 2 shows the MRC monthly DAOD climatology based on the 2003-2018 average as well
310 as the ratio of DAOD to total AOD for June-October over the tropical Atlantic. Climatologically
311 from June-October, the majority of airborne dust originates from the Sahara Desert, in contrast to
312 the winter season when a significant amount of dust is emitted over the Sahel and southern
313 Sahara (Engelstaedter [and](#) Washington, 2007). This dust is then transported westward over the
314 Atlantic and eventually to the Caribbean, largely within the 10-25°N latitude belt. The

315 transported African dust covers most of the Atlantic hurricane MDR, which spans the tropical
316 North Atlantic and Caribbean. The DAOD over the Atlantic is, on average, much higher in June,
317 July, and August (JJA) than in September and October because of higher emissions over the
318 African continent in the former months (Carlson and Prospero 1972; Engelstaedter and
319 Washington, 2007; Dunion [and](#) Marron, 2008; Dunion, 2011). DAOD is also much higher over
320 the tropical Atlantic than over the Caribbean, as dust aerosols are removed by wet and dry
321 processes during the long-range transport. The MRC shows that dust aerosols are the dominant
322 contributor to the total AOD in the MDR during most of the hurricane season (June–October).
323 The DAOD accounts for about 50–60% of the total AOD over the tropical North Atlantic and
324 around 30–50% over the Caribbean for JJA. This suggests that the total AOD can be a relatively
325 good indicator of DAOD in the tropical North Atlantic but is not as good of an indicator in the
326 Caribbean for JJA. The DAOD contribution to total AOD is about 10–20% less for September
327 and October. Considering the potential larger forcing by airborne dust in JJA than in September
328 and October, the focus season in this study is JJA.

329 As transport of Saharan dust across the Atlantic during summer is often associated with SAL
330 outbreaks, which are approximately centered around 700 hPa (Dunion [and](#) Velden, 2004;
331 Dunion, 2011), monthly climatological 700 hPa relative humidity (RH) and horizontal wind are
332 also shown in Figure 2. Climatologically, the MDR is dominated by the mid-level easterly jet (7–
333 8 m s⁻¹) during JJA and weaker easterlies (5–6 m s⁻¹) during September and October. Over the
334 Caribbean, the wind direction veers slightly towards the north for all of the studied months and
335 relates to this region being typically positioned on the west side of the climatological Atlantic
336 subtropical ridge. 700 hPa RH is on the order of 40% and 50% for the tropical Atlantic and the
337 Caribbean respectively for JJA and is about 10% higher in September and October. RH is higher
338 in the Caribbean than in the tropical North Atlantic as the impact of dry air from the SAL and
339 from upper-level subsidence becomes weaker from east to west. For context, the Atlantic moist
340 tropical sounding, defined in Dunion (2011), has average 700 hPa winds of 3.6 m s⁻¹ at 112°
341 (wind direction) and 66% RH, while the mean SAL sounding has corresponding values of 7.8 m
342 s⁻¹ at 91° and 34% RH.

343 Figure 3 shows the monthly mean AERONET version 3 L2 and MRC 550 nm modal AOD time
344 series at four AERONET sites that are primarily influenced by African dust. From east to west,
345 these sites include Dakar, Senegal (14.4°N, 17.0°W), Cape Verde (16.7°N, 22.9°W), Ragged
346 Point, Barbados (13.2°N, 59.4°W), and La Parguera, Puerto Rico (18.0°N, 67.0°W), which are
347 also marked in Figure 1. The boreal summer peak dust activity (i.e., JJA) is highlighted. Dust
348 aerosols are typically considered coarse-mode, although there may be a very small amount of
349 mass in fine-mode. The fine-mode AOD observed in AERONET measurements for these sites
350 are normally dominated by pollution and biomass-burning smoke. Dakar and Cape Verde
351 experience dust aerosols throughout the year, with a peak in JJA and a weaker secondary peak
352 during the boreal winter, which is associated with dust emissions from the Sahel. The Ragged
353 Point and La Parguera sites, which are remote receptor sites in the Caribbean, are influenced by
354 African dust predominantly during boreal summer, thus displaying a pronounced peak of total
355 and coarse-mode AODs in JJA. The secondary AOD peak during winter at Dakar and Cape
356 Verde is generally not observed at Ragged Point or La Parguera, as African dust is transported to
357 the south following the low-to-mid-level trade wind flow, occasionally reaching South America
358 (Prospero, 2014).

359 Figure 3 also shows the bias, the root mean square error (RMSE) of MRC and the correlation (r)
360 between MRC and AERONET for monthly AODs at each of the four AERONET sites. Overall,
361 MRC follows the seasonal and interannual variability in AERONET data for the total AOD quite
362 well, and to a slightly lesser extent for the coarse-mode AOD. Coarse-mode aerosols include dust
363 and sea salt, but are dominated by dust aerosols over the tropical North Atlantic for JJA (Figure
364 2c, speciated AOD cannot be obtained from AERONET measurements). The correlation is >0.9
365 for the coarse-mode AOD and tends to be better at the long-range transport sites (i.e., Ragged
366 Point and La Parguera) than the sites close to the dust source (i.e., Dakar and Cape Verde). The
367 correlation is slightly lower in the source area than in the long-range transport region because
368 there are large uncertainties in emissions and strong gradients due to local aerosol sources in the
369 source area. Also, the source area allows less time for AOD data assimilation to correct aerosol
370 mass loads, in addition to a lower signal/noise ratio of AOD retrievals over land than over water
371 (e.g., Levy et al., 2005). The small bias, low RMSE and the high correlation with AERONET
372 data illustrate the ability of MRC to capture the aerosol environment in the MDR. In addition, all
373 of the three individual aerosol reanalyses that form the foundation of MRC have similar
374 verification scores against AERONET, though the MRC typically has a better verification score
375 than the individual reanalyses (Table 1). If we were to give different qualitative ratings for the
376 three individual reanalyses for the study area, MERRA-2 is slightly better over North Africa and
377 NAAPS-RA is slightly better over the Caribbean in terms of coarse-mode and total AOD
378 RMSEs.

379 Figure 4 shows the time series of monthly mean and regionally-averaged DAOD from MRC and
380 the three contributing reanalyses from 2003-2018 for the tropical North Atlantic and Caribbean
381 as defined in Fig. 2. The DAODs from the three reanalyses have similar seasonal and interannual
382 variability and are highly correlated, with $r \geq 0.95$ for the entire 16-yr period and $r \geq 0.85$ for
383 JJA for both regions based on monthly means. The magnitudes of JJA DAOD from the three
384 individual reanalyses are comparable over the tropical North Atlantic, with a 20% maximum
385 difference among the three products based on JJA DAOD. The climatological average of JJA
386 DAOD over the tropical North Atlantic is 0.21. The difference can be as much as ~ 0.06 (a $\sim 60\%$
387 difference between member products) for the Caribbean. The climatological average of JJA
388 DAOD in the Caribbean is 0.10. Since the total and coarse-mode AOD verification statistics for
389 the three products at the Caribbean AERONET sites are similar (Table 1), the DAOD difference
390 is most likely due to the different partitioning of aerosol species (e.g., dust versus sea salt
391 aerosols) during the total AOD data assimilation process. This is related to the fact that total
392 AOD is the only aerosol property constrained by satellite observations through AOD data
393 assimilation in all three aerosol reanalysis products, while speciated AOD is not constrained
394 (Lynch et al., 2016; Randles et al., 2017; Inness et al., 2019). Nevertheless, the DAOD from the
395 MRC is likely the most reliable given the generally better performance of multi-aerosol model
396 consensus compared to individual aerosol models (Sessions et al., 2015; Xian et al., 2019).

397 **3.2 Relationship between North Atlantic TC activity and JJA DAOD**

398 Accumulated Cyclone Energy (ACE) is often utilized to represent TC activity and is defined to
399 be the square of the one-minute maximum sustained wind speed at each six-hourly interval when
400 a tropical or subtropical cyclone (with maximum sustained winds ≥ 34 kt) is present (Bell et al.,
401 2000). Basin-wide ACE is used here, as it is assumed that MDR conditions affect to some extent,
402 the ACE of all storms that pass through the MDR, including those that later moved out of the

403 MDR. For example, we hypothesize that in an active dust year, the suppressed conditions in the
404 MDR would make for weaker, less organized AEWs that have less of a chance for formation
405 even if they do eventually move out of the MDR. Later we show in Table 2 that using ACE
406 generated in the Caribbean domain yields a consistent (same sign) yet stronger correlation
407 relationship between DAOD and ACE.

408 Atlantic TC activity shows a statistically significant relationship with regionally-averaged
409 Caribbean JJA DAOD. Figure 5a displays this relationship, with higher Caribbean DAOD
410 correlating ($r = -0.61$ with MRC DAOD and r of similar magnitudes from all three individual
411 reanalyses and exceeding the two-tailed 95% statistical significance level) with quieter Atlantic
412 hurricane seasons as quantified by ACE. While tropical North Atlantic DAOD and Caribbean
413 DAOD in JJA correlate strongly ($r = 0.88$), Figure 5b shows that the relationship between
414 DAOD and ACE is weaker in the tropical North Atlantic than in the Caribbean. The correlation
415 between tropical North Atlantic DAOD and ACE is -0.41 , which falls below the statistical
416 significance threshold (correlations with MERRA-2 and CAMSRA DAODs are also
417 insignificant). We will show in the next section that the relationship between large-scale fields
418 known to impact Atlantic TC activity also tend to have higher correlations with JJA Caribbean
419 DAOD than with JJA tropical North Atlantic DAOD.

420 Given the strength of the relationship between Caribbean DAOD and seasonal Atlantic ACE, we
421 next investigate the relationship in extreme JJA DAOD seasons. We take the three seasons from
422 2003-2018 when JJA Caribbean DAOD was at its highest levels and when it was at its lowest
423 levels.

424 The three seasons with the highest JJA Caribbean DAOD were 2018, 2015 and 2014 in
425 descending order, and the three seasons with the lowest JJA Caribbean DAOD were 2005, 2011
426 and 2017 in ascending order based on MRC. The left column of Figure 6 shows DAOD
427 composites for the three high and the three low JJA Caribbean DAOD seasons and their
428 differences. DAOD is not only higher over the MDR in the high Caribbean DAOD seasons, but
429 dust aerosols are transported farther to the west. DAOD differences between the extreme high
430 and low DAOD seasons over the tropical North Atlantic and Caribbean are ~ 0.05 - 0.08 . In fact,
431 the three high dust years have roughly 60% more DAOD in the Caribbean than the three low
432 dust years (regional average of 0.13 vs. 0.08), while these differences are not as large in the
433 tropical North Atlantic. The transport pathway of dust is also shifted slightly to the south in the
434 tropical North Atlantic in the three high DAOD seasons.

435 The right column of Figure 6 displays the JJA-averaged 850 hPa winds and 700 hPa RH for the
436 three high and three low JJA Caribbean DAOD seasons, and the difference between these high
437 and low seasons. Large-scale conditions over the Caribbean during JJA were much less
438 conducive for TCs in the high DAOD seasons, with drier middle levels ($>10\%$ relative humidity
439 difference) and stronger easterly trade winds (2 - 4 m s^{-1} stronger), implying an overall less
440 hurricane-favorable dynamic and thermodynamic environment. This is consistent with the
441 depiction of the thermodynamic structure of the SAL by Dunion and Velden (2004). The
442 stronger AEJ associated with higher DAOD is also consistent with modeling studies when
443 aerosol radiative effects are taken into account (Tompkins et al., 2005). Associated with high
444 Caribbean DAOD, the position of the center of the Azores High was slightly shifted to the
445 southwest, which facilitates stronger dust transport into the Caribbean. This is in agreement with
446 the findings of Riemer and Doherty (2006) who suggested the importance of the position of the

447 Azores High in African dust transport across the Atlantic, although their study was only during
448 the boreal winter. As would be expected from these large-scale conditions, Atlantic TC activity
449 was much higher in low JJA Caribbean DAOD seasons.

450 Table 2 displays observed Atlantic TC activity as well as the ratios of observed average seasonal
451 Atlantic TC activity in the three low JJA Caribbean DAOD seasons versus the three high
452 Caribbean DAOD seasons. Atlantic basin-wide numbers of tropical depressions, named storms,
453 hurricanes, major (Category 3+ on the Saffir-Simpson Hurricane Wind Scale) hurricanes and
454 ACE are higher by a factor of ~1.9 - ~2.8 in the three low relative to the three high Caribbean
455 DAOD seasons. The ratios are even higher (e.g., 12 times higher for ACE) for TC activity in the
456 Caribbean. The 2018 Atlantic hurricane season was an interesting case, as it was an above-
457 average overall hurricane season (as measured by ACE), but much of the ACE that was
458 generated that year occurred outside of the tropics ($>23.5^{\circ}\text{N}$) (Saunders et al. 2020). Very little
459 activity occurred in the Caribbean in 2018.

460 In addition, the ratio for major hurricanes is higher than the ratios for tropical depressions,
461 named storms, and hurricanes, indicating a stronger relationship between dust aerosols and
462 intense storms than between dust aerosols and weak storms. A total of 17 major hurricanes were
463 observed in the Atlantic in the three low Caribbean DAOD seasons, compared with only 6 major
464 hurricanes in the three high Caribbean DAOD seasons. The three low Caribbean DAOD seasons
465 had six continental United States major hurricane landfalls (2005 Hurricanes Dennis, Katrina,
466 Rita, and Wilma and 2017 Hurricanes Harvey and Irma), while the three high Caribbean DAOD
467 seasons had one continental United States major hurricane landfall (2018 Hurricane Michael).

468 Figure 7 displays the named storm formation location of all Atlantic TCs in the three seasons
469 with the highest JJA Caribbean DAOD and the three seasons with the lowest Caribbean DAOD
470 along with the maximum intensity that these TCs reached. As would be expected from the
471 differences in large-scale conditions noted earlier, TCs that became major hurricanes formed
472 much more frequently south of 20°N in the three lowest Caribbean DAOD seasons than in the
473 three highest Caribbean DAOD seasons. These differences were most pronounced in the
474 Caribbean, with only one named storm (Hanna in 2014) forming in the Caribbean in the three
475 highest JJA Caribbean DAOD seasons. In the three lowest Caribbean JJA DAOD seasons, 11
476 named storms formed in the Caribbean.

477 **3.3 Relationship between JJA DAOD and large-scale atmosphere/ocean fields**

478 We next examine the relationship between JJA DAOD and large-scale atmosphere/ocean fields.
479 In this analysis, we begin by focusing on several fields that have been documented in prior
480 research to significantly impact Atlantic TC activity: 850 hPa zonal wind (850 hPa U), 200 hPa
481 zonal wind (200 hPa U), zonal wind shear between 200 hPa and 850 hPa, 700 hPa RH, 850 hPa
482 relative vorticity and SST (Gray, 1968; Saunders et al., 2017). More active Atlantic hurricane
483 seasons are typically associated with anomalous westerly 850 hPa U (e.g., weaker trade winds),
484 anomalous easterly 200 hPa U (counteracting prevailing upper-level westerlies) and thus weaker
485 wind shear, higher 850 hPa relative vorticity, higher mid-level relative humidity and
486 anomalously warm SSTs. We investigate the relationships with DAOD in the tropical North
487 Atlantic and the Caribbean as defined in Figure 2.

488 Figure 8 displays the correlation between regionally-averaged MRC JJA DAOD in the Caribbean
489 and the six large-scale fields just discussed. Higher JJA Caribbean DAOD is associated with
490 stronger 850 hPa easterly trades and increased 200 hPa upper-level westerlies (and hence
491 stronger vertical wind shear), drier air at 700 hPa and anomalously cool SST across the MDR.
492 Weaker 850 hPa relative vorticity also predominates over most of the Caribbean. However,
493 almost no correlation is found between Caribbean JJA DAOD and 850 hPa relative vorticity in
494 the tropical North Atlantic, possibly due to the counteracting role of covariability of African dust
495 emissions and AEWs - as was inferred from a positive correlation between the two by
496 Karyampudi and Carlson (1988). This result is also consistent with Figure 7 which shows more
497 named storms and therefore likely stronger AEW activity right off of the coast of west Africa
498 between 10-20°N in high dust DAOD years. This result reflects the complexity of the TC-dust
499 interaction relationship. In addition, the vorticity field is extremely noisy. Figure 8f is extended
500 to include the eastern and central tropical Pacific in order to investigate the potential relationship
501 between ENSO and DAOD, with Caribbean DAOD showing a significant positive relationship
502 with ENSO.

503 The relationship between the same six large-scale fields and JJA tropical North Atlantic DAOD
504 is considerably weaker, with lower correlations observed for all six fields (Figures S2). In
505 addition, the regions with significant correlations decrease in spatial extent relative to the
506 Caribbean DAOD correlations shown in Figure 8.

507 We next investigate Maximum Potential Intensity (MPI), an integrated TC index, which
508 combines a list of key factors (similar to those explored above). MPI assesses how conducive
509 atmospheric thermodynamic conditions are for TC intensification, providing a theoretical limit of
510 the strength of a TC (Holland, 1997; Bister and Emanuel, 1998). Figures 9a and c show the
511 correlations between the Caribbean region-averaged JJA DAOD and JJA/ASO MPI calculated
512 based on Bister and Emanuel (1998). Consistent with the results for the individual large-scale
513 fields, JJA MPI over the MDR exhibits strong negative correlations with JJA Caribbean DAOD
514 (~ -0.7, also Table 3). One of the primary inputs to the MPI calculation is SST, so the strong
515 inverse relationship between MPI and DAOD is expected given the strong inverse relationship
516 between SST and DAOD. The correlation is significant but weaker for ASO MPI for most of the
517 MDR, except for the eastern tropical North Atlantic, where the negative correlation drops below
518 statistical significance. The negative correlation of JJA/ASO MPI with JJA tropical North
519 Atlantic region-averaged DAOD is much weaker than that with JJA Caribbean DAOD in the
520 MDR (Figure 9b and d) and drops below statistical significance in the Caribbean.

521 The genesis potential index (GPI) is another integrated TC index that is often used to provide an
522 estimate of the potential for tropical cyclogenesis (e.g., Emanuel and Nolan, 2004; Camargo et
523 al., 2007). Monthly GPI is calculated following Emanuel and Nolan (2004). Figure 10 shows the
524 correlation between region-averaged JJA DAODs and JJA and ASO GPI. Consistent with the
525 results for the individual large-scale fields and MPI, JJA GPI over the MDR exhibits strong
526 negative correlations (~-0.7, also Table 3) with JJA Caribbean DAOD. Similar to MPI, GPI is
527 also directly related to SST via the potential intensity term, so given the negative correlation
528 between DAOD and SST, we would expect a negative correlation between GPI and DAOD.
529 Other terms also comprise the GPI, including vertical wind shear and mid-level moisture, which
530 also correlate negatively with DAOD. The correlation remains statistically significant but is
531 weaker for ASO GPI for most of the MDR. The exception is the eastern tropical North Atlantic,

532 where the negative correlation drops below 95% statistical significance. The negative correlation
533 of JJA/ASO GPI with JJA tropical North Atlantic region-averaged DAOD is much weaker than
534 that with JJA Caribbean DAOD in the MDR (Figure 10b and d), which is also consistent with the
535 result for the individual large-scale fields and MPI.

536 Table 3 summarizes the relationship between large-scale atmosphere/ocean fields, MPI, GPI, and
537 DAOD, with correlations displayed between JJA region-averaged DAOD and concurrent region-
538 averaged fields (i.e., JJA-averaged), as well as the large-scale region-averaged fields during the
539 peak of the Atlantic hurricane season from August-October. 850 hPa relative vorticity is
540 excluded as no statistically significant correlations are found. While the correlations between the
541 other five large-scale fields, MPI, GPI, and DAOD tend to weaken from JJA to ASO, the
542 correlations remain significant for all of these large-scale fields, and the integrated TC indices, in
543 the Caribbean during ASO. For the tropical North Atlantic, JJA DAOD has much weaker and
544 insignificant correlations with JJA 200 hPa zonal wind, wind shear and 700 hPa RH compared to
545 those for the Caribbean. However its negative correlation with SST is as strong as that for the
546 Caribbean in JJA and remains statistically significant from JJA to ASO, although the magnitude
547 of the correlation is weaker in ASO. These contribute to a negative correlation with MPI and GPI
548 and a stronger correlation during JJA than during ASO.

549 Part of the reason for the rapid decrease in the strength of the correlations in the tropical North
550 Atlantic is due to relatively low correlations between JJA and ASO values of large-scale
551 parameters in that portion of the basin, indicating a lack of persistence in atmosphere/ocean
552 conditions when compared with the Caribbean (Table 4). The persistence of the 700 hPa RH and
553 850 hPa U fields in the tropical North Atlantic is especially low compared to other fields.

554 **3.4 Relationship between JJA DAOD and large-scale climate modes**

555 We next explore the relationship between JJA-averaged DAOD and two large-scale climate
556 modes that have been documented in many studies to impact Atlantic TC activity: ENSO (e.g.,
557 Gray, 1984; Goldenberg [and](#) Shapiro, 1996; Klotzbach, 2011; Klotzbach et al., 2018) and the
558 AMM (e.g., Kossin [and](#) Vimont, 2007; Patricola et al., 2014). El Niño typically reduces
559 Atlantic TC activity through several mechanisms including increasing westerly wind shear
560 especially over the Caribbean (Gray, 1984) and through upper-level tropospheric warming,
561 causing increased static stability and inhibiting deep convection (Tang [and](#) Neelin, 2004). The
562 AMM has also been suggested in prior research to significantly impact Atlantic TC activity
563 (Kossin [and](#) Vimont, 2007), especially when combined with ENSO (Patricola et al., 2014). A
564 positive phase of the AMM is associated with a warmer than normal tropical Atlantic,
565 anomalously low sea level pressure and anomalously weak trade winds - all of which favor
566 Atlantic TC formation (Kossin [and](#) Vimont, 2007).

567 Table 5 displays the correlations between JJA regionally-averaged DAODs from the different
568 aerosol reanalysis products and the JJA and ASO ENSO (as represented by the ONI) and AMM
569 indices. There is a positive correlation between JJA Caribbean DAOD and the concurrent
570 (significant at the 90% level) and ASO ONI (significant at the 95% level) using MRC and
571 NAAPS-RA, and the correlations with the ONI increase from JJA to ASO. The correlation
572 between JJA tropical North Atlantic DAOD and JJA/ASO ENSO is not significant, however,
573 consistent with previous studies (Lau and Kim, 2007; Doherty et al., 2014). ENSO events
574 climatologically intensify from boreal summer to boreal autumn (Harrison [and](#) Larkin, 1998),

575 which may be part of the reason for the increase in significance of the correlations from JJA to
576 ASO. In addition, this likely also explains part of the reason why Atlantic TC activity correlates
577 more strongly with Caribbean DAOD than with tropical Atlantic DAOD, given the pronounced
578 impact that ENSO has on the Caribbean large-scale environment (Gray, 1984). Figure S3, in
579 which JJA composites of MRC DAOD, 850 hPa horizontal wind and 700 hPa RH for the three
580 top El Nino and La Nino ENSO years (based on JJA ONI) are shown, corroborates that stronger
581 dust transport into Caribbean occurs during El Nino years without necessarily strong emissions
582 over Africa and high DAOD over tropical North Atlantic. We also note that 2015 is both an El
583 Niño and a high DAOD year, while 2011 is both a La Niña and low DAOD year. Removing the
584 two overlapping years in the composites leads to similar results except that DAOD differences
585 between El Nino and La Nino years are more negative in the tropical North Atlantic, additionally
586 supporting the insignificant correlation between ENSO and tropical North Atlantic DAOD.

587 The correlations between JJA Caribbean DAOD and JJA AMM are consistently strong and
588 negative (~ -0.7) with all of the aerosol reanalyses (Table 5). As might be expected given that the
589 signal of the AMM is climatologically strongest in the boreal spring and weakens in the boreal
590 summer and fall (Kossin ~~&~~and Vimont, 2007), correlations of JJA DAOD are weaker with the
591 ASO AMM than with the JJA AMM. Negative correlations are also obtained between the JJA
592 tropical North Atlantic DAOD and the JJA AMM, while the correlation with the ASO AMM is
593 weak and not statistically significant in general. The negative correlations between JJA DAODs
594 and the AMM are consistent with Evan et al. (2011)'s study on the radiative effect of dust
595 aerosols on the AMM. That study showed DAOD to be not only negatively correlated with the
596 AMM but that its variability was found to excite the AMM on interannual to decadal time scales.

597 So far we have shown that Caribbean DAOD is correlated with Atlantic basin-wide ACE as well
598 as two-large scale climate modes: ENSO and the AMM. Both of these modes have been shown
599 to also impact Atlantic TC activity. To remove the influence of these climate indices from the
600 relationship between DAOD and ACE, we use partial correlation analysis (Sharma et al., 1978).
601 Table 6 shows the partial correlation matrix between JJA Caribbean and tropical North Atlantic
602 DAOD and annual Atlantic basin-wide ACE while controlling for the ONI and AMM indices,
603 respectively. Removing the influence of ENSO causes little change in the negative correlation
604 between MRC Caribbean JJA DAOD and ACE. The correlation remains statistically significant,
605 suggesting that ENSO is not primarily responsible for the negative correlation between
606 Caribbean DAOD and Atlantic ACE, at least during the study period. The correlation between
607 tropical North Atlantic JJA DAOD and ACE also changes little, although the correlation is weak
608 and not statistically significant initially. We note that the correlation between ONI and ACE is
609 very weak and is not significant during the 2003-2018 study period, partially due to the
610 extremely active 2004 Atlantic hurricane season which occurred despite a weak El Niño event.

611 In contrast to the findings of removing ENSO from the DAOD-ACE relationship, after removing
612 the influence of the AMM, the correlation between Caribbean JJA DAOD and Atlantic ACE is
613 much weaker and drops to insignificant levels, suggesting that the AMM is an important factor in
614 the dust-TC relationship. However, it is hard to argue that the AMM is the determining factor in
615 the dust-TC relationship, as the correlation of ACE with JJA Caribbean DAOD is slightly higher
616 than with the JJA AMM (-0.61 vs. 0.59). When the partial correlation is calculated between the
617 AMM and ACE while removing the Caribbean dust (DAOD) influence, the correlation drops
618 from 0.59 to an insignificant level ($r = -0.26$), independent of season examined. This indicates

619 that Caribbean DAOD is, in turn, an important factor in the AMM-TC relationship. When the
620 TATL JJA DAOD is removed, the correlation between AMM and ACE is also reduced, implying
621 that the AMM/DAOD/TC relationship is strongly intertwined. This is physically feasible, as the
622 dust radiative forcing can result in cooler SST, which can introduce anomalously high sea level
623 pressure and stronger trade winds (and therefore stronger vertical wind shear), which is
624 characteristic of a negative AMM. This air-sea coupled response to dust radiative forcing can act
625 over relatively short timescales (e.g., one to two months) (Evan et al. 2011). Additionally, the
626 dryness of the dusty air and the radiative heating of the dust layer, can lead to stronger vertical
627 wind shear and a more stable lower atmosphere, all in line with a negative AMM that creates an
628 environment that is detrimental for TC formation and development. It could be argued that the
629 negative correlation between DAOD and Atlantic TC activity may be a result of forcing of the
630 AMM by African dust.

631 **4. Sensitivity tests**

632 The sensitivity of our results to the domain definitions of the tropical North Atlantic and the
633 Caribbean regions is explored by defining equal areas (shifting the separation longitude to
634 52.5°W) for the two regions within the MDR, as well as by expanding the two regions by 5°
635 latitude to the north (e.g., to 25°N). Neither of the two new definitions for regions significantly
636 change the correlations between JJA regionally averaged DAOD and large-scale fields (Table
637 S1, S2). The correlations between the JJA Caribbean DAOD and ACE are -0.59/-0.58 for the
638 longitudinal and latitudinal shift respectively, only slightly lower than -0.61 using the default
639 regional definitions. The correlations between the JJA TATL DAOD and ACE remain
640 insignificant (Table S3).

641 While airborne dust can impact TC activity, once TCs form and develop, both precipitation and
642 strong winds can significantly remove these dust particles. However, the removal effect by TCs
643 cannot primarily explain the negative DAOD-TC relationship. This is because peak dust activity
644 occurs from June to August with larger DAOD in June and July than in August over the Atlantic,
645 suggesting that peak DAOD in general leads the peak TC season by ~1-2 months (Figure S1).
646 Using June-July average DAOD instead of June-August average DAOD changes our results only
647 slightly. For example, the correlation between June-July Caribbean DAOD and Atlantic ACE is -
648 0.58, only slightly lower than that using JJA DAOD ($r = -0.61$) (Table S3). This has implications
649 for using DAOD as an indicator for seasonal TC forecasts which are often updated in early
650 August.

651 The sensitivity of the composite analysis of high versus low JJA Caribbean DAOD years to the
652 number of years is also explored by using two and four years for composites in addition to three
653 years (Table S4). Consistent results are found across all sensitivity tests. Atlantic basin-wide
654 numbers of tropical depressions, named storms, hurricanes and major hurricanes, and ACE are
655 higher (by a factor of 1.6-5) in the low than in the high JJA Caribbean DAOD seasons. The ratios
656 of observed average seasonal Atlantic hurricanes and major hurricanes in the low versus the high
657 JJA Caribbean DAOD seasons are generally higher than those of tropical depressions and named
658 storms, suggesting a stronger correlation relationship between dust aerosols and intense storms
659 than weak storms.

660 **5. Conclusions and Discussions**

661 The relationship between African dust and Atlantic tropical cyclone (TC) activity has been
662 analyzed in many prior studies (e.g., Dunion ~~and~~ Velden 2004; Evan et al. 2006a; Braun et al.
663 2013; Pan et al. 2018). This study has revisited this relationship with a statistical analysis using
664 three newly available aerosol reanalyses: the Naval Aerosol Analysis and Prediction System
665 reanalysis (NAAPS-RA), the Modern-Era Retrospective analysis for Research and Applications,
666 Version 2 (MERRA-2) aerosol reanalysis, the Copernicus Atmosphere Monitoring Service
667 ReAnalysis (CAMSR), and a multi-reanalysis-consensus (MRC) based on the three reanalyses
668 for the period 2003-2018. The datasets are validated with ground-based observations for modal
669 (fine, coarse and total) aerosol optical depth (AOD). The MRC data is primarily used in this
670 study as it generally has better verification results than any of the individual reanalysis products.
671 To our knowledge, this is the first climate study using a multi-reanalysis consensus to represent
672 aerosol conditions. Our findings are summarized below:

- 673 1. Total AOD of the three aerosol reanalysis products are similar for the Atlantic Main
674 Development Region, however, AOD attributed to individual aerosol species (such as
675 dust aerosols) can be quite different among the three reanalysis products (Figure 4). June-
676 July-August (JJA) dust AOD (DAOD) magnitude can differ by as much as 0.06,
677 corresponding to approximately 60% of the climatological JJA DAOD based on MRC for
678 the Caribbean, and can differ by as much as 0.05, approximately 20% of the
679 climatological JJA DAOD based on MRC for the tropical North Atlantic. This is because
680 total AOD is the only aerosol property constrained by satellite observations through AOD
681 data assimilation in all three aerosol reanalysis products, while speciated AOD is not
682 constrained. This also supports the potential usefulness of MRC, as multi-model-
683 consensus are found to generally be better performers than individual models in aerosol
684 simulations (Sessions et al., 2015; Xian et al., 2019). Despite differences in DAOD
685 magnitude, DAODs of the three reanalysis products correlate significantly over the
686 tropical Atlantic and Caribbean.
- 687 2. Each of the three individual reanalyses and the MRC have significant and negative
688 correlations between JJA Caribbean DAOD and seasonal Atlantic Accumulated Cyclone
689 Energy (ACE) (Table 2). High JJA DAOD in the Caribbean is associated with a less
690 conducive environment for hurricane activity as represented by cooler SST, enhanced
691 vertical wind shear, lower mid-level moisture, and by lower Maximum Potential Intensity
692 (MPI) and Genesis Potential Index (GPI) values (Table 3). Pronounced differences in
693 Atlantic TC activity are seen when examining the three seasons with the highest levels of
694 JJA Caribbean DAOD compared with the three seasons with the lowest JJA Caribbean
695 DAOD (Table 4 and Figure 7). About three times as many major hurricanes occurred
696 during the three lowest DAOD seasons (2005, 2011, 2017) compared with the three
697 highest DAOD seasons (2018, 2015, 2014). Atlantic TC activity is also negatively
698 correlated with tropical North Atlantic DAOD but not as significantly as with Caribbean
699 DAOD for possible reasons discussed in the conclusion that follows.
- 700 3. High Caribbean DAOD is typically associated with El Niño conditions, however ENSO
701 does not appear to significantly impact the Caribbean DAOD-ACE relationship. The
702 robust DAOD-ACE correlation still holds after removing ENSO's influence via partial
703 correlation analysis.

704 4. JJA north Atlantic DAOD and the Atlantic Meridional Mode (AMM) are intertwined in
705 the dust-TC relationship. Both the Caribbean and tropical North Atlantic DAODs have
706 strong negative correlations with JJA values of the AMM index (with a stronger
707 correlation for the Caribbean DAOD). Meanwhile, the JJA AMM index correlates
708 significantly with Atlantic ACE. For AMM and DAOD, removing the other in their
709 relationships with ACE dramatically reduces the significance of the correlations based on
710 partial correlation analysis. This result supports Evan et al.(2011)'s work, which showed
711 that African dust excited AMM variability on interannual to decadal time scales through
712 radiative forcing of the underlying SST. Consequently, it can be argued that the negative
713 correlation between Caribbean and tropical North Atlantic DAOD and Atlantic TC
714 activity may be a result of forcing of the AMM by African dust.

715 These results agree with previous studies that showed negative correlations between boreal
716 summer Atlantic dustiness and TC activity (e.g., Dunion and Velden, 2004; Evan et al., 2006a;
717 Lau and Kim 2007). The correlations obtained in this study, especially those with Caribbean
718 DAOD, are slightly higher than previous studies, including correlations between boreal summer
719 dustiness and ACE (Evan et al., 2006a; Lau and Kim 2007) and between JJA dustiness and
720 ENSO (DeFlorio et al., 2016). We note that the study areas, time periods and study methods are
721 not identical between our study and these previous studies, implying the usefulness of aerosol
722 reanalyses in climate studies. Various sensitivity tests show that our results are not sensitive to
723 the definitions of areas for the Caribbean and tropical North Atlantic, the number of composite
724 years used, or the definition of the dust season (June-July vs. June-August).

725 Our results also document statistically significant relationships between Atlantic dustiness and
726 large-scale fields (e.g., SST, vertical wind shear, mid-level moisture and relatively vorticity) and
727 integrated TC diagnostic indices (e.g., MPI and GPI), which can be seen as confounding factors
728 in the dust-TC relationship. Exploring the causality of the documented negative correlation
729 between DAOD and Atlantic TC activity through modeling experiments is beyond the scope of
730 this paper. However in some modeling studies, radiative forcing of the scattering dust alone
731 could result in an inverse relationship between African dust and Atlantic TC activity (Dunstone
732 et. al, 2013; Strong et al., 2018; Sobel et al., 2019), along with consistent large-scale fields
733 associated with TC activity. So it is possible that radiative forcing of the scattering dust is a
734 dominant factor in the inverse dust-TC relationship on seasonal-interannual and basin-wide
735 scales. After all, aerosols are coupled radiatively with meteorology in the ERA-Interim dataset,
736 which provides the large-scale atmospheric data used in this study.

737 The correlations with Atlantic ACE are higher for Caribbean DAOD than for tropical North
738 Atlantic DAOD - a result that was not documented previously. The differences in the
739 relationships of Atlantic ACE with regional DAOD are potentially due to several factors:

740 a) The large-scale environmental fields investigated herein are better self-correlated
741 between the JJA and ASO seasons over the Caribbean than over the tropical North Atlantic
742 (Table 4). Therefore, the higher correlation with JJA Caribbean DAOD, which reflects the large-
743 scale circulation, especially for the low- and mid-level wind flow that modulates how far African
744 dust can be transported, tends to extend into the ASO peak TC season. As was shown in
745 Saunders et al. (2017), the strength of the low-level winds in the Caribbean tends to be the most
746 robust diagnostic for seasonal ACE during the peak months of the Atlantic hurricane season.

747 b) ENSO has a large impact on the Caribbean large-scale environment (Gray, 1984). ENSO-
748 forced SST anomalies typically exhibit very strong persistence from JJA to ASO (Harrison ~~&~~and
749 Larkin, 1998). As Caribbean JJA DAOD is correlated with ENSO to some extent, it is also
750 correlated with Atlantic ACE.

751 c) There might be a regime shift in the integrated outcome of dust-TC interactions from east
752 to west across the tropical North Atlantic at climate time scales, with the eastern tropical North
753 Atlantic (e.g., close to the African continent) having a positive correlation (e.g., since dust
754 emission is often associated with AEWs emerging from Africa; Jones et al., 2003; Karyampudi
755 and Carlson, 1988) while the correlation becomes more negative heading west across the basin.

756 d) The relatively larger JJA DAOD variability in the Caribbean (larger relative dynamical
757 range of Caribbean JJA DAOD compared to the tropical north Atlantic JJA DAOD over 2003-
758 2018) could contribute to a higher correlation (Figures 3 and 4).

759 e) AOD data quality is comparatively better over the Caribbean than over the tropical north
760 Atlantic (Table 1; Figure 3), given that AOD reanalyses generally perform better over long-range
761 transport regions than they do closer to the aerosol source regions (Xian et al., 2016).

762 The conclusions drawn from this study are based on 16-year records (2003-2018) of DAOD data
763 from the MRC. We acknowledge that this analysis represents a relatively short timespan for a
764 climate correlation study. Longer-period aerosol reanalyses with good fidelity are needed for
765 further climate studies. These reanalyses face several challenges including dealing with changes
766 to the network of AOD-observing satellites over time, as well as reasonable simulations and
767 partitioning of aerosol-speciated AODs associated with rare severe aerosol events (e.g., volcanic
768 eruptions) within AOD data assimilation systems.

769 It is also worth noting that the 2003-2018 DAOD climatology for the Atlantic MDR could be
770 low relative to the extremely dusty period of the 1980s that has been documented by long-term
771 in-situ dust concentration measurements made in Barbados (Prospero, 2014) and a 24-year
772 eastern North Atlantic dust cover record derived from the Advanced Very High Resolution
773 Radiometer (AVHRR, Evan et al., 2006). Dust concentration records at Barbados (1965-2011)
774 and dust cover determined from AVHRR (1982-2005) both indicate that dust levels over the
775 North Atlantic peaked during the mid-1980s, when tropical Atlantic TC activity was relatively
776 low (e.g., Wang et al., 2012). Our findings are consistent with the negative correlations reflected
777 in both the earlier dust and the earlier tropical Atlantic TC activity records.

778 Since we note that JJA/JJ Caribbean DAOD are strongly correlated with large-scale atmospheric
779 fields which are frequently used in seasonal hurricane forecasts, DAOD may be a useful
780 confirmation tool for observed thermodynamic conditions. Most groups issuing seasonal
781 hurricane forecasts provide an update in early August (immediately prior to the peak of the
782 Atlantic hurricane season). So early season (June-July) DAOD, especially over the Caribbean,
783 could be a potential indicator for the strength of seasonal Atlantic TC activity. While there is
784 very strong agreement between large-scale zonal wind fields (e.g., the June-July-averaged 850
785 hPa zonal wind over the tropical Atlantic correlates at 0.92 between ERA-Interim and MERRA-
786 2, in which impact of aerosols on radiation and thereby on meteorology is included), there is less
787 agreement with the mid-level moisture field. The correlation between ERA-Interim and
788 MERRA-2 700 hPa RH over the tropical Atlantic averaged over June-July is only 0.72. The

789 DAOD could potentially be used to help clarify the favorability/unfavorability of the
790 thermodynamic environment, as indicated also by the strong correlation between JJA Caribbean
791 DAOD and JJA and ASO MPI.

792 We believe this study, which shows a robust correlation relationship for the integrated dust-
793 atmosphere-ocean system, could provide a framework to better understand the linkages between
794 DAOD and Atlantic TC activity and how DAOD affects the large-scale environment of the
795 MDR. ~~This~~We find that DAOD in both the tropical Atlantic and Caribbean is negatively
796 correlated with Atlantic hurricane frequency, intensity and integrated indices such as ACE, with
797 stronger negative correlations in the Caribbean than farther east in the tropical North Atlantic.
798 However, this study focuses on seasonal to interannual time scales and provides ~~aspects~~analysis
799 from a large-scale point of view. Finer temporal scales (from hours to days) are needed in future
800 studies for cases where African dust is entrained into TC vortices.

801 **Acknowledgments:**

802 NAAPS-RA development and application and authors P. Xian and J.S. Reid are supported by the
803 Office of Naval Research Code 322. P. Klotzbach would like to acknowledge a grant from the G.
804 Unger Vetlesen Foundation. P. Colarco is supported by the NASA Modeling, Analysis, and
805 Prediction program (program manager: David Considine).

806 **Data Availability:** All data supporting the conclusions of this manuscript are available through
807 the links provided below:

808 AERONET Version 3 Level 2 data: <http://aeronet.gsfc.nasa.gov>

809 AMM index:

810 <https://www.esrl.noaa.gov/psd/data/timeseries/monthly/AMM/ammsst.data>

811 CAMSRA AOD: <https://www.ecmwf.int/en/research/climate-reanalysis/cams-reanalysis>

812 ENSO index:

813 http://origin.cpc.ncep.noaa.gov/products/analysis_monitoring/ensostuff/ONI_v5.php

814 ERA-interim monthly means: <https://rda.ucar.edu/datasets/ds627.1/>

815 HURDAT2:

816 <https://www.aoml.noaa.gov/hrd/hurdat/hurdat2.html>

817 MERRA-2 AOD:

818 https://disc.gsfc.nasa.gov/datasets/M2TMNXAER_V5.12.4/summary?keywords=%22MERRA-2%22

819 NAAPS RA AOD: [https://usgodae.org/cgi-](https://usgodae.org/cgi-bin/datalist.pl?dset=nrl_naaps_reanalysis&summary=Go)

820 [bin/datalist.pl?dset=nrl_naaps_reanalysis&summary=Go](https://usgodae.org/cgi-bin/datalist.pl?dset=nrl_naaps_reanalysis&summary=Go)

821 NOAA OI SST V2 data: <https://www.esrl.noaa.gov/psd/>

822 **Author contribution:** P. J. K, J. P. D. and P.X. conceived the idea. P.X. and P.J.K performed
823 most of the analysis and writing. M.A.J. calculated and performed the analyses on MPI and GPI.
824 All authors contributed to the writing and revision of the manuscript.

825 **Competing interests:** The authors declare that they have no conflict of interest.

826 **References**

832 Barnston, A. G., Chelliah, M., ~~&and~~ Goldenberg, S. B. ~~(1997)~~.: Documentation of a highly
833 ENSO-related SST region in the equatorial Pacific. *Atmosphere-Ocean*, 35(3), 367-383.
834 <https://doi.org/10.1080/07055900.1997.9649597>, 1997.

835 Bell, G. D., Halpert, M. S., Schnell, R. C., Higgins, R. W., Lawrimore, J., Kousky, V. E., et al.
836 ~~(2000)~~.: Climate assessment for 1999. *Bulletin of the American Meteorological Society*, 81(6),
837 S1-S50. [https://doi.org/10.1175/1520-0477\(2000\)81\[s1:CAF\]2.0.CO;2](https://doi.org/10.1175/1520-0477(2000)81[s1:CAF]2.0.CO;2), 2000.

838 Bercos-Hickey, E., Nathan, T. R., and Chen, S. H. ~~(2017)~~.: Saharan dust and the African easterly
839 jet-African easterly wave system: Structure, location and energetics. *Quarterly Journal of the*
840 *Royal Meteorological Society*, 143(708), 2797-2808. <https://doi.org/10.1002/qj.3128>, 2017.

841 Bister, M., and Emanuel, K. A. ~~(2002)~~.: Low frequency variability of tropical cyclone potential
842 intensity. 1. Interannual to interdecadal variability. *J. Geophys. Res.*, 107, 4801,
843 doi:10.1029/2001JD000776., 2002.

844 Braun, S. A., Sippel, J. A., Shie, C.-L., ~~&and~~ Boller, R. A. ~~(2013)~~.: The evolution and role of the
845 Saharan air layer during Hurricane Helene (2006). *Monthly Weather Review*, 141(12), 4269–
846 4295. <https://doi.org/10.1175/MWR-D-13-00045.1>, 2013.

847 Braun, S. A. ~~(2010)~~.: Re-evaluating the role of the Saharan Air Layer in Atlantic tropical
848 cyclogenesis and evolution. *Monthly Weather Review*, 138(6), 2007–2037.
849 <https://doi.org/10.1175/2009MWR3135.1>, 2010.

850 Bretl, S., Reutter, P., Raible, C. C., Ferrachat, S., Poberaj, C. S., Revell, L. E., ~~&and~~ Lohmann, U.
851 ~~(2015)~~.: The influence of absorbed solar radiation by Saharan dust on hurricane genesis. *Journal*
852 *of Geophysical Research: Atmospheres*, 120(5), 1902–1917.
853 <https://doi.org/10.1002/2014JD022441>, 2015.

854 Buchard, V., Randles, C. A., da Silva, A., Darmenov, A. S., Colarco, P. R., Govindaraju, R.C., et
855 al., ~~(2017)~~.: The MERRA-2 Aerosol Reanalysis, 1980-onward, Part II: Evaluation and case
856 studies. *Journal of Climate*, 30(17), 6851-6872. <https://doi.org/10.1175/JCLI-D-16-0613.1>, 2017.

857 Carlson, T. N., ~~&and~~ Prospero, J. M. ~~(1972)~~.: The large-scale movement of Saharan air
858 outbreaks over the northern equatorial Atlantic. *Journal of Applied Meteorology*, 11(2), 283–
859 297. [https://doi.org/10.1175/1520-0450\(1972\)011<0283:TLSMOS>2.0.CO;2](https://doi.org/10.1175/1520-0450(1972)011<0283:TLSMOS>2.0.CO;2), 1972.

860 Camargo, S. J., Emanuel, K. A. ~~&and~~ Sobel, A. H. ~~(2007)~~.: Use of a genesis potential index to
861 diagnose ENSO effects on tropical cyclone genesis. *J. Clim.*, 20, 4819–4834, 2007.

862 Chin, M., Rood, R., Lin, S., Muller J., ~~&and~~ Thompson, A. ~~(2000)~~.: Atmospheric sulfur cycle
863 simulated in the global model GOCART: Model description and global properties. *Journal of*
864 *Geophysical Research: Atmospheres*, 105(D20), 24,671–24,687.
865 <https://doi.org/10.1029/2000JD900384>, 2000.

866 Colarco, P. R., Toon, O. B., Reid, J. S., Livingston, J. M., Russell, P. B., Redemann, J., et al.,
867 ~~(2003)~~.: Saharan dust transport to the Caribbean during PRIDE: 2. Transport, vertical profiles,
868 and deposition in simulations of in situ and remote sensing observations. *Journal of Geophysical*
869 *Research: Atmospheres*, 108(D19), 8590, <https://doi.org/10.1029/2002JD002659>, 2003.

870 Colarco, P., da Silva, A., Chin, M., ~~&and~~ Diehl, T. ~~(2010)~~.: Online simulations of global aerosol
871 distributions in the NASA GEOS-4 model and comparisons to satellite and ground-based aerosol
872 optical depth. *Journal of Geophysical Research: Atmospheres*, 115(D14207),
873 <https://doi.org/10.1029/2009JD012820>, 2010.

874 Dee, D. P., Uppala, S. M., Simmons, A. J., Berrisford, P., Poli, P., Kobayashi, S., Andrae, U., et
875 al. ~~(2011)~~.: The ERA-Interim reanalysis: configuration and performance of the data assimilation
876 system. *Quarterly Journal of the Royal Meteorological Society*, 137(656), 553-597.
877 <https://doi.org/10.1002/qj.828>, 2011.

Formatted: Font: Not Italic

Formatted: No underline

Formatted: Font: Not Italic

Formatted: No underline

Formatted: Font: Not Italic

Formatted: No underline

Formatted: Font: Not Italic

Formatted: Font: Not Italic

Formatted: No underline

Formatted: Font: Not Italic

Formatted: No underline

Formatted: Font: Not Italic

Formatted: Font: Not Italic

Formatted: No underline

Formatted: Font: Not Italic

Formatted: No underline

Formatted: Font: Not Italic

Formatted: Font: Not Bold

Formatted: Font: Not Italic

Formatted: Font: Not Italic

Formatted: No underline

Formatted: Font: Not Italic

Formatted: No underline

Formatted: Font: Not Italic

Formatted: No underline

878 DeFlorio, M. J., Goodwin, I. D., Cayan, D. R., Miller, A. J., Ghan, S. J., Pierce, D. W., Russell,
879 L. M., et al. ~~(2016)~~. Interannual modulation of subtropical Atlantic boreal summer dust
880 variability by ENSO. *Climate Dynamics*, 46(1), 585-599. [https://doi.org/10.1007/s00382-015-
882 2600-7](https://doi.org/10.1007/s00382-015-

881 2600-7), 2016.

882 DeMott, P., Sassen, K., Poellot, M., Baumgardner, D., Rogers, D., Brooks, S. D., Prenni, A. J.,
883 &and Kreidenweis, S. M. ~~(2003)~~. African dust aerosols as atmospheric ice nuclei. *Geophysical*
884 *Research Letters*, 30, 1732. <https://doi.org/10.1029/2003GL017410>, 2003.

885 Doherty, O. M., Riemer, N., &and Hameed, S. ~~(2008)~~. Saharan mineral dust transport into the
886 Caribbean: Observed atmospheric controls and trends. *Journal of Geophysical Research:*
887 *Atmospheres*, 113(D07211). <https://doi.org/10.1029/2007JD009171>, 2008.

888 Dunion, J. P. ~~(2011)~~. Re-writing the climatology of the tropical North Atlantic and Caribbean
889 Sea atmosphere. *Journal of Climate*, 24(3), 893–908. <https://doi.org/10.1175/2010JCLI3496.1>,
890 2011.

891 Dunion, J. P., &and Marron, C. S. ~~(2008)~~. A reexamination of the Jordan mean tropical
892 sounding based on awareness of the Saharan air layer: Results from 2002. *Journal of Climate*,
893 21(20), 5242–5253. <https://doi.org/10.1175/2008JCLI1868.1>, 2008.

894 Dunion, J. P., &and Velden, C. S. ~~(2004)~~. The impact of the Saharan Air Layer on Atlantic
895 tropical cyclone activity. *Bulletin of the American Meteorological Society*, 85(3), 353-365.
896 <https://doi.org/10.1175/BAMS-85-3-353>, 2004.

897 Emanuel, K. A., &and Nolan, D. S. ~~(2004)~~. Tropical cyclone activity and global climate. In:
898 *Proc. of 26th Conference on Hurricanes and Tropical Meteorology*, pp. 240–241, American
899 Meteorological Society, Miami, FL., 2004.

900 Engelstaedter, S., &and Washington, R. ~~(2007)~~. Atmospheric controls on the annual cycle of
901 North African dust. *Journal of Geophysical Research: Atmospheres*, 112(D3), D03103.
902 <https://doi.org/10.1029/2006JD007195>, 2007.

903 Evan, A.T., Dunion, J. P., Foley, J. A., Heidinger, A. K., &and Velden, C. S. ~~(2006a)~~. New
904 evidence for a relationship between Atlantic tropical cyclone activity and African dust outbreaks.
905 *Geophysical Research Letters*, 33, L19813. <https://doi.org/10.1029/2006GL026408>, 2006a.

906 Evan, A. T., Heidinger, A. K., &and Knippertz P. ~~(2006b)~~. Analysis of winter dust activity off
907 the coast of West Africa using a new 24-year over-water advanced very high resolution
908 radiometer satellite dust climatology. *Journal of Geophysical Research: Atmospheres*, 111(D12),
909 D12210. <https://doi.org/10.1029/2005JD006336>, 2006b.

910 Evan, A. T., Foltz, G. R., Zhang, D., &and Vimont D. J. ~~(2011)~~. Influence of African dust on
911 ocean–atmosphere variability in the tropical Atlantic. *Nature Geoscience*.4, 762–765.
912 <https://doi.org/10.1038/ngeo1276>, 2011.

913 Evan, A. T., Vimont, D. J., Heidinger, A. K., Kossin, J. P., &and Bennartz, R. ~~(2009)~~. The role
914 of aerosols in the evolution of tropical North Atlantic Ocean temperature anomalies. *Science*,
915 324(5928), 778-781. <https://doi.org/10.1126/science.1167404>, 2009.

916 Flemming, J., Benedetti, A., Inness, A., Engelen, R. J., Jones, L., Huijnen, V., Remy, S.,
917 Parrington, M., Suttie, M., Bozzo, A., Peuch, V.-H., Akritidis, D., and Katragkou, E.: The
918 CAMS interim Reanalysis of Carbon Monoxide, Ozone and Aerosol for 2003–2015, *Atmos.*
919 *Chem. Phys.*, 17, 1945–1983, <https://doi.org/10.5194/acp-17-1945-2017>, 2017.

920 Giles, D. M., Sinyuk, A., Sorokin, M. G., Schafer, J. S., Smirnov, A., Slutsker, I., Eck, T. F., et
921 al. ~~(2019)~~. Advancements in the Aerosol Robotic Network (AERONET) Version 3 database –
922 automated near-real-time quality control algorithm with improved cloud screening for Sun

Formatted: Font: Not Italic

Formatted: No underline

Formatted: Font: Not Italic

Formatted: Font: Not Italic

Formatted: No underline

Formatted: Font: Not Italic

Formatted: No underline

923 photometer aerosol optical depth (AOD) measurements. *Atmospheric Measurement Techniques*,
924 12(1), 169-209, <https://doi.org/10.5194/amt-12-169-2019>, 2019.

925 Goldenberg, S. B., Landsea, C. W., Mestas-Núñez, A. M., & Gray, W. M. (2001). The
926 recent increase in Atlantic hurricane activity: Causes and implications. *Science*, 293(5529), 474-
927 479. <https://doi.org/10.1126/science.1060040>, 2001.

928 Goldenberg, S. B., & Shapiro, L. J. (1996). Physical mechanisms for the association of El
929 Niño and West African rainfall with Atlantic major hurricane activity. *Journal of Climate*, 9(6),
930 1169-1187. [https://doi.org/10.1175/1520-0442\(1996\)009%3C1169:PMFTAO%3E2.0.CO;2](https://doi.org/10.1175/1520-0442(1996)009%3C1169:PMFTAO%3E2.0.CO;2),
931 1996.

932 Gray, W. M. (1968). Global view of the origin of tropical disturbances and storms. *Monthly*
933 *Weather Review*, 96(10), 669-700. [https://doi.org/10.1175/1520-0493\(1968\)096%3C0669:GVOTOO%3E2.0.CO;2](https://doi.org/10.1175/1520-0493(1968)096%3C0669:GVOTOO%3E2.0.CO;2), 1968.

934 Gray, W. M. (1984). Atlantic seasonal hurricane frequency. Part I: El Niño and 30 mb quasi-
935 biennial oscillation influences. *Monthly Weather Review*, 112(9), 1649-1668.
936 [https://doi.org/10.1175/1520-0493\(1984\)112%3C1649:ASHFPI%3E2.0.CO;2](https://doi.org/10.1175/1520-0493(1984)112%3C1649:ASHFPI%3E2.0.CO;2), 1984.

937 Grogan, D. F. P., Nathan, T. R., Chen, S. H. (2016). Effects of Saharan dust on the linear
938 dynamics of African easterly waves. *Journal of Atmospheric Science*, 73(2), 891-911.
939 <https://doi.org/10.1175/JAS-D-15-0143.1>, 2016.

940 Grogan, D. F. P., Nathan, T. R., Chen, S. H. (2017). Saharan dust and the nonlinear evolution
941 of the African easterly jet-African easterly wave system. *Journal of Atmospheric Science*, 74(1),
942 27-47. <https://doi.org/10.1175/JAS-D-16-0118.1>, 2017.

943 Harrison, D. E., Larkin, N. K. (1998). El Niño-Southern Oscillation sea surface temperature and
944 wind anomalies, 1946-1993. *Reviews of Geophysics*, 36(3), 353-400.
945 <https://doi.org/10.1029/98RG00715>, 1998.

946 Herbener, S. R., van den Heever, S. C., Carriro, G. G., Saleeby, S. M., Cotton W. R. (2014).
947 Aerosol indirect effect on idealized tropical cyclone dynamics. *Journal of Atmospheric Science*,
948 71, 2040-2055. <https://doi.org/10.1175/JAS-D-13-0202.1>, 2014.

949 Herbener, S. R., S. M. Saleeby, S. C. van den Heever, S. C., and Twohy, C. H. Twohy
950 (2016). Tropical storm redistribution of Saharan dust to the upper troposphere and ocean
951 surface, *Geophys. Res. Lett.*, 43, doi:10.1002/2016GL070262, 2016.

952 Holben, B. N., Eck, T. F., Slutsker, I., Tanre, D., Buis, J. P., Setzer, A., et al. (1998).
953 AERONET - A federated instrument network and data archive for aerosol characterization,
954 *Remote Sensing of the Environment*, 66(1), 1-16. [https://doi.org/10.1016/S0034-4257\(98\)00031-5](https://doi.org/10.1016/S0034-4257(98)00031-5),
955 1998.

956 Holben, B. N., Tanré, D., Smirnov, A., Eck, T. F., Slutsker, I., Abuhassan, N., et al. (2001). An
957 emerging ground-based aerosol climatology: Aerosol optical depth from AERONET, *Journal of*
958 *Geophysical Research: Atmospheres*, 106(D11), 12067-12097.
959 <https://doi.org/10.1029/2001JD900014>, 2001.

960 Holland, G. J., 1997. The maximum potential intensity of tropical cyclones. *J. Atmos. Sci.*, 54,
961 2519-2541, [https://doi.org/10.1175/1520-0469\(1997\)054<2519:TMPIOT>2.0.CO;2](https://doi.org/10.1175/1520-0469(1997)054<2519:TMPIOT>2.0.CO;2), 1997.

962 Hsu, N. C., Gautam, R., Sayer, A. M., Bettenhausen, C., Li, C., Jeong, M. J., et al. (2012).
963 Global and regional trends of aerosol optical depth over land and ocean using SeaWiFS
964 measurements from 1997 to 2010. *Atmospheric Chemistry and Physics*, 12, 8037-8053.
965 <https://doi.org/10.5194/acp-12-8037-2012>, 2012.

966 Hyer, E. J., Reid, J. S., & Zhang, J. (2011). An over-land aerosol optical depth data set for
967 data assimilation by filtering, correction, and aggregation of MODIS Collection 5 optical depth

Formatted: Font: Not Italic

Formatted: Font: Not Italic

Formatted: Font: Not Italic

Formatted: No underline

Formatted: Font: Not Italic

Formatted: Font: Not Italic

Formatted: No underline

969 retrievals. *Atmospheric Measurement Techniques*, 4(3), 379-408. [https://doi.org/10.5194/amt-4-](https://doi.org/10.5194/amt-4-379-2011)
970 [379-2011](https://doi.org/10.5194/amt-4-379-2011), 2011.

971 Inness, A., Baier, F., Benedetti, A., Bouarar, I., Chabrilat, S., Clark, H., Clerbaux, C., Coheur,
972 P., Engelen, R. J., Errera, Q., Flemming, J., George, M., Granier, C., Hadji-Lazaro, J., Huijnen,
973 V., Hurtmans, D., Jones, L., Kaiser, J. W., Kapsomenakis, J., Lefever, K., Leitão, J., Razinger,
974 M., Richter, A., Schultz, M. G., Simmons, A. J., Suttie, M., Stein, O., Thépaut, J.-N., Thouret,
975 V., Vrekoussis, M., Zerefos, C., and the MACC team: The MACC reanalysis: an 8 yr data set of
976 atmospheric composition, *Atmos. Chem. Phys.*, 13, 4073–4109, [https://doi.org/10.5194/acp-13-](https://doi.org/10.5194/acp-13-4073-2013)
977 [4073-2013](https://doi.org/10.5194/acp-13-4073-2013), 2013.

978 Inness, A., Ades, M., Agustí-Panareda, A., Barré, J., Benedictow, A., Blechschmidt, A.-M.,
979 Dominguez, J. J., Engelen, R., Eskes, H., Flemming, J., Huijnen, V., Jones, L., Kipling, Z.,
980 Massart, S., Parrington, M., Peuch, V.-H., Razinger, M., Remy, S., Schulz, M., and Suttie, M.:
981 The CAMS reanalysis of atmospheric composition, *Atmos. Chem. Phys.*, 19, 3515–3556,
982 <https://doi.org/10.5194/acp-19-3515-2019>, 2019.

983 Jenkins, G. S., Pratt, A. S. & Heymsfield, A. (2008). Possible linkages between Saharan
984 dust and tropical cyclone rain band invigoration in the eastern Atlantic during NAMMA-06.
985 *Geophysical Research Letters*, 35, L08815. <https://doi.org/10.1029/2008GL034072>, 2008.

986 Jones, T. A., Cecil, D. J. & Dunion, J. (2007). The environmental and inner-core conditions
987 governing the intensity of Hurricane Erin (2001). *Weather and Forecasting*, 22(4), 708–725.
988 <https://doi.org/10.1175/WAF1017.1>, 2007.

989 Jones, C., Mahowald, N. M., & Luo, C. (2003). The role of easterly waves on African desert
990 dust transport. *Journal of Climate*, 16, 3617–3628, 2003

991 Jones, C., Mahowald, N. M., & Luo, C. (2004). Observational evidence of African desert
992 dust intensification of easterly waves. *Geophysical Research Letters*, 31(17), L17208.
993 <https://doi.org/10.1029/2004GL020107>, 2004.

994 Joyce, R. J., Janowiak, J. E., Arkin, P. A., Xie, P. (2004). CMORPH: A method that produces
995 global precipitation estimates from passive microwave and infrared data at high spatial and
996 temporal resolution. *Journal of Hydrometeorology*, 5(3), 487–503, [https://doi.org/10.1175/1525-](https://doi.org/10.1175/1525-7541(2004)005%3C0487:CAMTPG%3E2.0.CO;2)
997 [7541\(2004\)005%3C0487:CAMTPG%3E2.0.CO;2](https://doi.org/10.1175/1525-7541(2004)005%3C0487:CAMTPG%3E2.0.CO;2), 2004.

998 Kahn, R. A., & Gaitley, B. J. (2015). An analysis of global aerosol type as retrieved by
999 MISR. *Journal of Geophysical Research: Atmospheres*, 120(9), 4248–4281.
1000 <https://doi.org/10.1002/2015JD023322>, 2015.

1001 Kaku, K. C., Reid, J. S., O'Neill, N. T., Quinn, P. K., Coffman, D. J., & Eck, T. F. (2014).
1002 Verification and application of the extended spectral deconvolution algorithm (SDA+)
1003 methodology to estimate aerosol fine and coarse mode extinction coefficients in the marine
1004 boundary layer. *Atmospheric Measurement Techniques*, 7(10), 3399–3412.
1005 <https://doi.org/10.5194/amt-7-3399-2014>, 2014.

1006 Karyampudi, V. M., & Carlson, T. N. (1988). Analysis and numerical simulations of the
1007 Saharan air layer and its effect on easterly wave disturbances. *Journal of the Atmospheric*
1008 *Sciences*, 45(21), 3102–3136. [https://doi.org/10.1175/1520-](https://doi.org/10.1175/1520-0469(1988)045<3102:AANSOT>2.0.CO;2)
1009 [0469\(1988\)045<3102:AANSOT>2.0.CO;2](https://doi.org/10.1175/1520-0469(1988)045<3102:AANSOT>2.0.CO;2), 1988.

1010 Karyampudi, V. M., & Pierce, H. F. (2002). Synoptic-scale influence of the Saharan Air
1011 Layer on tropical cyclogenesis over the eastern Atlantic. *Monthly Weather Review*, 130, 3100–
1012 3128, 2002.

1013 Karydis, V. A., Kumar, P., Barahona, D., Sokolik, I. N. & Nenes, A. (2011). On the effect
1014 of dust particles on global cloud condensation nuclei and cloud droplet number. *Journal of*

Formatted: Font: Not Italic

Formatted: No underline

Formatted: Font: Not Italic

Formatted: No underline

Formatted: Font: Not Italic

Formatted: No underline

Formatted: Font: Not Italic

Formatted: Font: Not Italic

Formatted: No underline

Formatted: Font: Not Italic

Formatted: Font: Not Italic

015 Geophysical Research: Atmospheres, 116(D23204). <https://doi.org/10.1029/2011JD016283>,
016 [2011](https://doi.org/10.1029/2011JD016283).

017 Khain, A. P., Leung, L. R., Lynn, B., ~~&and~~ Ghan, S. ~~(2009)~~: Effects of aerosols on the
018 dynamics and microphysics of squall lines simulated by spectral bin and bulk parameterization
019 schemes. *Journal of Geophysical Research: Atmospheres*, 114(D22203).
020 <https://doi.org/10.1029/2009JD011902>~~https://doi.org/10.1029/2009JD011902~~, 2009.

021 Klotzbach, P. J. ~~(2011)~~: El Niño – Southern Oscillation’s impact on Atlantic basin hurricanes
022 and U.S. landfalls. *Journal of Climate*, 24(4), 1252-1263.
023 <https://doi.org/10.1175/2010JCLI3799.1>, 2011.

024 Klotzbach, P. J., Bowen, S. G., Pielke Jr., R., Bell, M. M. ~~(2018)~~: Continental United States
025 landfall frequency and associated damage. Observations and future risks. *Bulletin of the*
026 *American Meteorological Society*, 99(7), 1359-1376. [https://doi.org/10.1175/BAMS-D-17-](https://doi.org/10.1175/BAMS-D-17-0184.1)
027 [0184.1](https://doi.org/10.1175/BAMS-D-17-0184.1), 2018.

028 Knippertz, P., Todd, M. C. ~~(2010)~~: The central west Saharan dust hot spot and its relation to
029 African easterly waves and extratropical disturbances. *Journal of Geophysical Research:*
030 *Atmospheres*, 115(D12117). <https://doi.org/10.1029/2009JD012819>, 2010.

031 Kossin, J. P., ~~&and~~ Vimont, D. J. ~~(2007)~~: A more general framework for understanding Atlantic
032 hurricane variability and trends. *Bulletin of the American Meteorological Society*, 88(11), 1767–
033 1782. <https://doi.org/10.1175/BAMS-88-11-1767>, 2007.

034 Kuciauskas, A. P., Xian, P., Hyer, E. J., Oyola, M. I. ~~&and~~ Campbell, J. R. ~~(2018)~~: Supporting
035 weather forecasters in predicting and monitoring Saharan Air Layer dust events as they impact
036 the Greater Caribbean. *Bulletin of the American Meteorological Society*, 99(2), 259-268.
037 <https://doi.org/10.1175/BAMS-D-16-0212.1>, 2018.

038 Landsea, C. W. ~~(1993)~~: A climatology of intense (or major) Atlantic hurricanes. *Monthly*
039 *Weather Review*, 121(6), 1703-1713. [https://doi.org/10.1175/1520-](https://doi.org/10.1175/1520-0493(1993)121%3C1703:ACOIMA%3E2.0.CO;2)
040 [0493\(1993\)121%3C1703:ACOIMA%3E2.0.CO;2](https://doi.org/10.1175/1520-0493(1993)121%3C1703:ACOIMA%3E2.0.CO;2), 1993.

041 Landsea, C. W., ~~&and~~ Franklin, J. L. ~~(2013)~~: Atlantic hurricane database uncertainty and
042 presentation of a new database format. *Monthly Weather Review*, 141(10), 3576-3592.
043 <https://doi.org/10.1175/MWR-D-12-00254.1>, 2013.

044 Lau, W. K. M., ~~&and~~ Kim, K. ~~(2007)~~: How nature foiled the 2006 hurricane forecasts. *Eos*
045 *Transactions American Geophysical Union*, 88(9), 105-107.
046 <https://doi.org/10.1029/2007EO090002>, 2007.

047 Levy, R. C., et al. ~~(2005)~~: Evaluation of the MODIS aerosol retrievals over ocean and land
048 during CLAMS. *J. Atmos. Sci.*, 62(4), 974–992, 2005.

049 Levy, R. C., Remer, L. A., Kleidman, R. G., Mattoo, S., Ichoku, C., Kahn, R., ~~&and~~ Eck, T. F.
050 ~~(2010)~~: Global evaluation of the Collection 5 MODIS dark-target aerosol products over land.
051 *Atmospheric Chemistry and Physics*, 10(21), 10399-10420. [https://doi.org/10.5194/acp-10-](https://doi.org/10.5194/acp-10-10399-2010)
052 [10399-2010](https://doi.org/10.5194/acp-10-10399-2010), 2010.

053 Lynch, P., Reid, J. S., Westphal, D. L., Zhang, J., Hogan, T. F., Hyer, E. A., et al. ~~(2016)~~: An
054 11-year global gridded aerosol optical thickness reanalysis (v1.0) for atmospheric and climate
055 sciences. *Geoscientific Model Development*, 9(4), 1489-1522. [https://doi.org/10.5194/gmd-9-](https://doi.org/10.5194/gmd-9-1489-2016)
056 [1489-2016](https://doi.org/10.5194/gmd-9-1489-2016), 2016.

057 Ma, P. L., Zhang, K., Shi, J. J., Matsui, T., ~~&and~~ Arking, A. ~~(2012)~~: Direct radiative effect of
058 mineral dust on the development of African easterly waves in late summer, 2003–07. *Journal of*
059 *Applied Meteorology and Climatology*, 51(12), 2090–2104. [https://doi.org/10.1175/JAMC-D-](https://doi.org/10.1175/JAMC-D-11-0215.1)
060 [11-0215.1](https://doi.org/10.1175/JAMC-D-11-0215.1), 2012.

Formatted: No underline

Formatted: Font: Not Italic

Formatted: Underline, Font color: Blue

Formatted: No underline

Formatted: Font: Not Italic

Formatted: No underline

Formatted: Font: Not Italic

Formatted: No underline

Formatted: Font: Not Italic

Formatted: No underline

Formatted: Font: Not Italic

Formatted: No underline

Formatted: Font: Not Italic

Formatted: Font: Not Italic

Formatted: Font: Not Italic

Formatted: No underline

Formatted: Font: Not Italic

Formatted: No underline

Formatted: Font: Not Italic

Formatted: No underline

Formatted: No underline

Formatted: Font: Not Italic

Formatted: Font: Not Italic

Formatted: Font: Not Italic

Formatted: No underline

Formatted: No underline

Formatted: Font: Not Italic

Formatted: No underline

Formatted: No underline

Formatted: Font: Not Italic

Formatted: No underline

061 Miller, R. L., ~~&and~~ Tegen, I. ~~(1998)~~: Climate response to soil dust aerosols. *Journal of Climate*,
062 11(12), 3247–3267. [https://doi.org/10.1175/1520-0442\(1998\)011<3247:CRTSDA>2.0.CO;2](https://doi.org/10.1175/1520-0442(1998)011<3247:CRTSDA>2.0.CO;2),
063 ~~1998~~.
064 Nathan, T. R., Grogan, D. F. P., ~~&and~~ Chen, S. H. ~~(2017)~~: Subcritical destabilization of African
065 easterly waves by Saharan mineral dust. *Journal of the Atmospheric Sciences*, 74(4), 1039–1055.
066 <https://doi.org/10.1175/JAS-D-16-0247.1>, 2017.
067 Nowotnick, E. P., Colarco, P. R., Braun, S. A., Barahona, D. O., da Silva, A., Hlavka, D. L., et
068 al. ~~(2018)~~: Dust impacts on the 2012 Hurricane Nadine track during the NASA HS3 field
069 campaign. *Journal of the Atmospheric Sciences*, 75(7), 2473–2489. [https://doi.org/10.1175/JAS-](https://doi.org/10.1175/JAS-D-17-0237.1)
070 [D-17-0237.1](https://doi.org/10.1175/JAS-D-17-0237.1), 2018.
071 Nowotnick, E., Colarco, P., da Silva, A., Hlavka, D., ~~&and~~ McGill, M. ~~(2014)~~: The fate of
072 Saharan dust across the Atlantic and implications for a central American dust barrier.
073 *Atmospheric Chemistry and Physics*, 11(16), 8415–8431. [https://doi.org/10.5194/acp-11-8415-](https://doi.org/10.5194/acp-11-8415-2011)
074 [2011](https://doi.org/10.5194/acp-11-8415-2011), 2011.
075 O'Neill, N. T., Eck, T. F., Smirnov, A., Holben, B. N., ~~&and~~ Thulasiraman, S. ~~(2003)~~: Spectral
076 discrimination of coarse and fine mode optical depth. *Journal of Geophysical Research:*
077 *Atmospheres*, 108(D17), 4559. <https://doi.org/10.1029/2002JD002975>, 2003.
078 Pan, B., Wang, Y., Hu, J., Lin, Y., Hsieh, J-S., Logan, T. et al., ~~(2018)~~: Impacts of Saharan
079 dust on Atlantic regional climate and implications for tropical cyclones. *Journal of Climate*,
080 31(18), 7621–744. [https://doi.org/10.1175/JCLI-D-16-](https://doi.org/10.1175/JCLI-D-16-0776.1)
081 [0776.1](https://doi.org/10.1175/JCLI-D-16-0776.1), 2018.
082 Patricola, C. M., Saravanan, R., ~~&and~~ Chang, P. ~~(2014)~~: The impact of the El Niño-Southern
083 Oscillation and Atlantic Meridional Mode on seasonal Atlantic tropical cyclone activity. *Journal*
084 *of Climate*, 27(14), 5311–5328. <https://doi.org/10.1175/JCLI-D-13-00687.1>, 2014.
085 Pratt, A. S., ~~&and~~ Evans, J. L. ~~(2008)~~: Potential impacts of the Saharan Air Layer on numerical
086 model forecasts of North Atlantic tropical cyclogenesis. *Weather and Forecasting*, 24(2), 420–
087 435. <https://doi.org/10.1175/2008WAF2007090.1>, 2008.
088 Prospero, J. M. ~~(1999)~~: Long-term measurements of the transport of African mineral dust to the
089 southeastern United States: Implications for regional air quality. *Journal of Geophysical*
090 *Research: Atmospheres*, 104(D13), 15917–15927. <https://doi.org/10.1029/1999JD900072>, 1999.
091 Prospero, J. M. ~~(2014)~~: Characterizing the temporal and spatial variability of African dust over
092 the Atlantic. *Past Global Changes Magazine*, 22(2), 68–69.
093 <https://doi.org/10.22498/pages.22.2.68>, 2014.
094 Prospero, J. M., ~~&and~~ Lamb, P. J. ~~(2003)~~: African droughts and dust transport to the Caribbean:
095 Climate change implications. *Science*, 302(5647), 1024–1027.
096 <https://doi.org/10.1126/science.1089915>, 2003.
097 Prospero, J. M., ~~&and~~ Nees, R. T. ~~(1986)~~: Impact of the North African drought and El Niño on
098 mineral dust in the Barbados trade winds. *Nature*, 320, 735. <https://doi.org/10.1038/320735a0>,
099 1986.
100 Randles, C. A., daSilva, A. M., Buchard, V., Colarco, P. R., Darmenov, A., Govindaraju, R., et
101 al. ~~(2017)~~: The MERRA-2 aerosol reanalysis, 1980 onward. Part I: System description and data
102 assimilation evaluation. *Journal of Climate*, 30(17), 6823–6850. [https://doi.org/10.1175/JCLI-D-](https://doi.org/10.1175/JCLI-D-16-0609.1)
103 [16-0609.1](https://doi.org/10.1175/JCLI-D-16-0609.1), 2017.
104 Reale, O., Lau, W. K., Kim, K. M., ~~&and~~ Brin, E. ~~(2009)~~: Atlantic tropical cyclogenetic
105 processes during SOP-3 NAMMA in the GEOS-5 global data assimilation and forecast system.

Formatted: Font: Not Italic

Formatted: No underline

Formatted: Font: Not Italic

Formatted: Font: Not Italic

Formatted: Font: Not Italic

Formatted: No underline

Formatted: Font: Not Italic

Formatted: Font: Not Italic

Formatted: No underline

Formatted: Font: Not Italic

Formatted: No underline

Formatted: Font: Not Italic

Formatted: No underline

Formatted: Font: Not Italic

106 Journal of Atmospheric Sciences, 66(12), 3563–3578. <https://doi.org/10.1175/2009JAS3123.1>,
107 2009.

108 Reale, O., Lau, K. M. &and da Silva, A. (2011): Impact of interactive aerosol on the African
109 easterly jet in the NASA GEOS-5 global forecasting system. Weather and Forecasting, 26(4),
110 504–519. <https://doi.org/10.1175/WAF-D-10-05025.1>, 2011.

111 Reed, K. A., Bacmeister, J. T., Huff, J. J. A., Wu, X., Bates, S. C., &and Rosenbloom, N. A.
112 (2019): Exploring the impact of dust on North Atlantic hurricanes in a high-resolution climate
113 model. Geophysical Research Letters, 46, 1105–1112. <https://doi.org/10.1029/2018GL080642>,
114 2019.

115 Reid, J. S., Kinney, J. E., Westphal, D. L., Holben, B. N., Welton, E. J., Tsay, S-C., et al-
116 (2003): Analysis of measurements of Saharan dust by airborne and ground-based remote
117 sensing methods during the Puerto Rico Dust Experiment (PRIDE). Journal of Geophysical
118 Research: Atmospheres, 108, 8586. <https://doi.org/10.1029/2002JD002493>, 2003.

119 Reynolds, R.W., Rayner, N. A., Smith, T. M., Stokes, D. C., &and Wang, W. (2002): An
120 improved in situ and satellite SST analysis for climate. Journal of Climate, 15(13), 1609–1625.
121 [https://doi.org/10.1175/1520-0442\(2002\)015<1609:AIISAS>2.0.CO;2](https://doi.org/10.1175/1520-0442(2002)015<1609:AIISAS>2.0.CO;2), 2002.

122 Riemer, N., O. M.-Doherty, O. M., and S.-Hameed (2006), S.: On the variability of African dust
123 transport across the Atlantic, Geophys. Res. Lett., 33, L13814, doi:10.1029/2006GL026163,
124 2006.

125 Rienecker, M. M., Suarez, M. J., Gelaro, R., Todling, R., Bacmeister, J., Liu, E., et al. (2011):
126 MERRA: NASA’s Modern Era Retrospective Analysis for Research and Applications. Journal of
127 Climate, 24(14), 3624-3648. <https://doi.org/10.1175/JCLI-D-11-00015.1>, 2011.

128 Rosenfeld, D., Khain, A., Lynn, B., &and Woodley, W. L. (2007): Simulation of hurricane
129 response to suppression of warm rain by sub-micron aerosols. Atmospheric Chemistry and
130 Physics, 7(13), 3411-3424. <https://doi.org/10.5194/acp-7-3411-2007>, 2007.

131 Sassen, K., DeMott, P. J., Prospero, J. M. &and Poellot, M. R. (2003): Saharan dust storms and
132 indirect aerosol effects on clouds: CRYSTAL-FACE results. Geophysical Research Letters,
133 30(12), 1633. <https://doi.org/10.1029/2003GL017371>, 2003.

134 Saunders, M. A., Klotzbach, P. J., &and Lea, A. S. (2017): Replicating annual North Atlantic
135 hurricane activity 1878-2012 from environmental variables. Journal of Geophysical Research:
136 Atmospheres, 122(12), 6284-6297. <https://doi.org/10.1002/2017JD026492>, 2017.

137 Saunders, M. A., Klotzbach, P. J., Lea, A. S. R., Schreck, C. J., &and Bell, M. M. (2020):
138 Quantifying the probability and causes of the surprisingly active 2018 North Atlantic hurricane
139 season. Manuscript submitted to Earth and Space Science, 7(3), 1-14,
140 <https://doi.org/10.1029/2019EA000852>, 2020.

141 Sessions, W. R., Reid, J. S., Benedetti, A., Colarco, P. R., da Silva, A., Lu, S., Sekiyama, T.,
142 Tanaka, T. Y., Baldasano, J. M., Basart, S., Brooks, M. E., Eck, T. F., Iredell, M., Hansen, J. A.,
143 Jorba, O. C., Juang, H.-M. H., Lynch, P., Morcrette, J.-J., Moorithi, S., Mulcahy, J., Pradhan, Y.,
144 Razinger, M., Sampson, C. B., Wang, J., and Westphal, D. L. (2015): Development towards a
145 global operational aerosol consensus: basic climatological characteristics of the International
146 Cooperative for Aerosol Prediction Multi-Model Ensemble (ICAP-MME), Atmos. Chem. Phys.,
147 15, 335-362, 2015.

148 Sharma, S.S., Kleinbaum, D.G., &and Kupper, L.L. (1978): Applied Regression Analysis and
149 Other Multivariate Methods. <https://doi.org/10.2307/3150614>, 1978.

150 Shi, Y., Zhang, J., Reid, J. S., Holben, B., Hyer, E. J., &and Curtis, C. (2011): An analysis of
151 the collection 5 MODIS over-ocean aerosol optical depth product for its implication in aerosol

Formatted: No underline

Formatted: Font: Not Italic

Formatted: No underline

Formatted: No underline

Formatted: Font: Not Italic

Formatted: No underline

Formatted: Font: Not Italic

Formatted: Font: Not Italic

Formatted: No underline

Formatted: Font: Not Italic

Formatted: Font: Not Italic

Formatted: No underline

Formatted: Font: Not Italic

Formatted: Font: Open Sans, 10.5 pt,

Formatted: No underline

152 assimilation, *Atmospheric Chemistry and Physics*, 11(2), 557-565. [https://doi.org/10.5194/acp-](https://doi.org/10.5194/acp-11-557-2011)
153 [11-557-2011](https://doi.org/10.5194/acp-11-557-2011), 2011.

154 Sippel, J. A., Braun, S. A., & Shie, C.-L. (2011). Environmental influences on the strength
155 of Tropical Storm Debby (2006). *Journal of the Atmospheric Sciences*, 68(11), 2557–2581.
156 <https://doi.org/10.1175/2011JAS3648.1>, 2011.

157 Strong, J. D. O., Vecchi, G. A., & Ginoux, P. (2018). The climatological effect of
158 Saharan dust on global tropical cyclones in a fully coupled GCM. *Journal of Geophysical*
159 *Research: Atmospheres*, 123, 5538–5559. <https://doi.org/10.1029/2017JD027808>, 2018.

160 Sobel, A. H., Camargo, S. J. and Previdi, M. (2019). Aerosol vs. greenhouse gas effects on
161 tropical cyclone potential intensity and the hydrologic cycle. *Journal of Climate*,
162 doi:10.1175/JCLI-D-18-0357.1, 2019.

163 Sun, D., Lau, K. M., & Kafatos, M. (2008). Contrasting the 2007 and 2005 hurricane
164 seasons: Evidence of possible impacts of Saharan dry air and dust on tropical cyclone activity in
165 the Atlantic basin. *Geophysical Research Letters*, 35, L15405.
166 <https://doi.org/10.1029/2008GL034529>, 2008.

167 Tang, B.H., & Neelin, J. D. (2004). ENSO influence on Atlantic hurricanes via tropospheric
168 warming. *Geophysical Research Letters*, 31(24), L24204.
169 <https://doi.org/10.1029/2004GL021072>, 2004.

170 Tompkins A. M., Cardinali, C., Morcrette, J. J., & Rodwell, M. (2005). Influence of aerosol
171 climatology on forecasts of the African easterly jet. *Geophysical Research Letters*, 32(10),
172 L10801. <https://doi.org/10.1029/2004GL022189>, 2005.

173 Tsamalis, C., Chedin, A., Pelon, J., & Capelle, V. (2013). The seasonal vertical distribution
174 of the Saharan Air Layer and its modulation by the wind. *Atmospheric Chemistry and Physics*,
175 13(22), 11235–11257. <https://doi.org/10.5194/acp-13-11235-2013>, 2013.

176 Towhy, C. H., Kreidenweis, S. M., Eidhammer, T., Browell, E.V., Heymsfield A. J., Bansemmer,
177 A. R., et al. (2009). Saharan dust particles nucleate droplets in eastern Atlantic clouds.
178 *Geophysical Research Letters*, 36, L01807. <https://doi.org/10.1029/2008GL035846>, 2009.

179 Wang, C., Dong, S., Evan, A. T., Foltz, G. R., & Lee, S. (2012). Multidecadal covariability
180 of North Atlantic sea surface temperature, African dust, Sahel rainfall and Atlantic hurricanes.
181 *Journal of Climate*, 25(15), 5404–5415. <https://doi.org/10.1175/JCLI-D-11-00413.1>, 2012.

182 Westphal, D. L., Toon, O. B., and Carlson, T. N. (1987). A two-dimensional numerical
183 investigation of the dynamics and microphysics of Saharan dust storms. *Journal of Geophysical*
184 *Research: Atmospheres*, 92, 3027 – 3049. <https://doi.org/10.1029/JD092iD03p03027>, 1987.

185 Wilcox, E. M., Lau, K. M., & Kim, K. M. (2010). A northward shift of the North Atlantic
186 Ocean intertropical convergence zone in response to summertime Saharan dust outbreaks.
187 *Geophysical Research Letters*, 37(4), L04804. <https://doi.org/10.1029/2009GL041774>, 2010.

188 Xian, P., Reid, J. S., Turk, J. F., Hyer, E. J., & Westphal, D. L. (2009). Impact of modeled
189 versus satellite measured tropical precipitation on regional smoke optical thickness in an aerosol
190 transport model. *Geophysical Research Letters*, 36, L16805.
191 <https://doi.org/10.1029/2009GL038823>, 2009.

192 Xian, P., Reid, J. S., Hyer, E. J., Sampson, C. R., Rubin, J. I., Ades, M., et al. (2019). Current
193 State of the global operational aerosol multi-model ensemble: an update from the International
194 Cooperative for Aerosol Prediction (ICAP). *Quarterly Journal of the Royal Meteorological*
195 *Society*. Published online Feb 4, 2019. <https://doi.org/10.1002/qj.3497>, 2019.

Formatted: Font: Not Italic

Formatted: No underline

Formatted: Font: Not Italic

Formatted: No underline

Formatted: Font: Not Italic

Formatted: Font: Not Italic

Formatted: No underline

Formatted: Font: Not Italic

1196 Zhang, H., McFarquhar, G. M., Cotton, W. R., ~~&and~~ Deng, Y. ~~(2009)~~.: Direct and indirect impacts
1197 of Saharan dust acting as cloud condensation nuclei on tropical cyclone eyewall development.
1198 Geophysical Research Letters, 36, L06802. <https://doi.org/10.1029/2009GL037276>. 2009.
1199 Zhang, H., McFarquhar, G. M., Saleeby, S. M., ~~&and~~ Cotton, W. R. ~~(2007)~~.: Impacts of Saharan
1200 dust as CCN on the evolution of an idealized tropical cyclone. Geophysical Research Letters, 34,
1201 L14812. <https://doi.org/10.1029/2007GL029876>. 2007.
1202 Zhang, J., ~~&and~~ Reid, J. S. ~~(2006)~~.: MODIS aerosol product analysis for data assimilation:
1203 Assessment of over-ocean level 2 aerosol optical thickness retrievals. Journal of Geophysical
1204 Research: Atmospheres, 111(D22207). <https://doi.org/10.1029/2005JD006898>. 2006.
1205 Zhang, J., ~~J. S.~~ Reid, J. S., R. Alfaro-Contreras, R. and ~~P.~~ Xian ~~(2017)~~. P. : Has China been
1206 exporting less particulate air pollution over the past decade?, Geophys. Res. Lett., 44, 2941–
1207 2948, doi:10.1002/
1208 2017GL072617-. 2017.

Formatted: Font: Not Italic

Formatted: No underline

Formatted: Font: Not Italic

Formatted: Font: Not Italic

Formatted: No underline

Formatted: Font: Not Bold

Formatted: Line spacing: single

1216 **Tables:**

1217

1218 **Table 1.** Root mean square error of total AOD (left number in each cell) and coarse-mode AOD
 1219 (right number in each cell) at 550nm from individual aerosol reanalyses, including CAMSRA,
 1220 MERRA-2, NAAPS-RA, and the Multi-Reanalysis-Consensus (MRC) verified with AERONET
 1221 V3L2 monthly data for the 2003-2018 time period. The rank of MRC among all reanalyses in
 1222 terms of RMSE is also shown. “~” means there are ties in the ranking. The first five sites are
 1223 located in North Africa or off of the northwestern coast of Africa. The last four sites are located
 1224 in or near the Caribbean Sea. AOD time series of MRC and AERONET at Dakar, Capo Verde,
 1225 Ragged Point and La Parguera sites are presented in Figure 3.

Site	CAMSRA	MERRA-2	NAAPS-RA	MRC	Rank of MRC
Banizoumbou	0.13 0.17	0.10 0.10	0.11 0.13	0.10 0.11	~1 2
Capo Verde	0.07 0.07	0.06 0.05	0.06 0.07	0.06 0.06	~1 2
Dakar	0.07 0.11	0.07 0.07	0.08 0.10	0.06 0.08	1 2
La Laguna	0.06 0.05	0.06 0.05	0.06 0.05	0.05 0.04	1 1
Santa Cruz Tenerife	0.04 0.04	0.04 0.04	0.04 0.04	0.03 0.03	1 1
Ragged Point	0.05 0.03	0.03 0.03	0.03 0.03	0.04 0.03	3 ~1
La Parguera	0.05 0.02	0.03 0.02	0.03 0.02	0.03 0.02	~1 ~1
Guadeloupe	0.05 0.05	0.05 0.04	0.04 0.05	0.04 0.04	~1 ~1
Key Biscayne	0.05 0.03	0.03 0.02	0.02 0.02	0.03 0.02	2 ~1

Formatted Table

1226

1227

1228 **Table 2.** Annual average Atlantic TC activity in the three seasons with the highest JJA
 1229 Caribbean DAOD (2014, 2015 and 2018) and the three seasons with the lowest JJA Caribbean
 1230 DAOD (2005, 2011 and 2017). Ratios between the three low and the three high DAOD seasons
 1231 are also provided. Corresponding numbers for the Caribbean are provided in parentheses next to
 1232 the total basin-wide numbers.

	Tropical Depressions and Named Storms	Named Storms	Hurricanes	Major Hurricanes	Accumulated Cyclone Energy
Three highest JJA Caribbean DAOD	12.3 (2.3)	11.3 (2.3)	6.0 (0.3)	2.0 (0.0)	86 (3)
Three lowest JJA Caribbean DAOD	23.0 (6.7)	21.3 (6.7)	10.7 (3.0)	5.7 (2.7)	199 (39)
Ratio	1.9 (2.9)	1.9 (3.0)	1.8 (9.0)	2.8 (N/A)	2.3 (13.0)

Formatted Table

1233

1234

1235

1236 **Table 3.** Correlation matrix between regionally-averaged multi-reanalysis-consensus (MRC) JJA
 1237 tropical North Atlantic/Caribbean DAOD and 850 hPa U, 200 hPa U, 200 hPa minus 850 hPa U
 1238 (zonal wind shear), 700 hPa RH, SST, Maximum Potential Intensity (MPI) and Genesis Potential
 1239 Index (GPI) during JJA and ASO, respectively. Correlations that are statistically significant at
 1240 the 90% level are highlighted in bold and those with asterisks are statistically significant at the
 1241 95% level. 850 hPa relative vorticity is not shown as none of these correlations were statistically
 1242 significant.

Environmental Field	JJA tropical North Atlantic / JJA Caribbean	ASO tropical North Atlantic / ASO Caribbean
850 hPa U	-0.63* / -0.79*	0.03 / -0.66*
200 hPa U	0.34 / 0.81*	0.30 / 0.85*
200 minus 850 hPa U	0.43 / 0.83*	0.22 / 0.82*
700 hPa RH	-0.43 / -0.80*	-0.34 / -0.55*
SST	-0.71* / -0.75*	-0.44 / -0.79*
MPI	-0.74* / -0.68*	-0.47 / -0.67*
GPI	-0.75* / -0.76*	-0.62* / -0.69*

Formatted Table

1243

1244

1245

1246 **Table 4.** Correlation matrix between JJA and ASO values of 850 hPa U, 200 hPa U, 200 minus
1247 850 hPa U, 700 hPa RH and SST over the tropical North Atlantic and the Caribbean,
1248 respectively. Correlations that are statistically significant at the 90% level are highlighted in
1249 bold, and those with asterisks are statistically significant at the 95% level.

Environmental Field	Tropical North Atlantic	Caribbean
850 hPa U	0.51*	0.84*
200 hPa U	0.71*	0.88*
200 minus 850 hPa U	0.72*	0.90*
700 hPa RH	0.48	0.74*
SST	0.77*	0.85*

Formatted Table

1250

1251

1252 **Table 5:** Correlations of MRC JJA Caribbean DAOD or JJA tropical North Atlantic (TATL)
 1253 DAOD with the JJA or ASO Oceanic Nino Index (ONI) and the AMM. Correlations that are
 1254 statistically significant at the 90% level are highlighted in bold. Correlations that are statistically
 1255 significant at the 95% level are marked with *.

	JJA Caribbean DAOD				JJA TATL DAOD			
	CAMSRA	MERRA-2	NAAPS-RA	MRC	CAMSRA	MERRA-2	NAAPS-RA	MRC
JJA ONI	0.33	0.29	0.50	0.44	0.24	0.18	0.28	0.26
ASO ONI	0.42	0.41	0.61*	0.54*	0.38	0.30	0.42	0.41
JJA AMM	-0.72*	-0.70*	-0.63*	-0.76*	-0.58*	-0.65*	-0.36	-0.60*
ASO AMM	-0.42	-0.45	-0.30	-0.45	-0.33	-0.52*	0.01	-0.33

Formatted Table

1256

1257

1258

1259 **Table 6.** Partial correlation matrix between MRC JJA Caribbean and tropical North Atlantic
 1260 (TATL) DAOD and annual Atlantic basin-wide ACE while controlling for ENSO (using the JJA
 1261 ONI) and the AMM (using JJA AMM index). Linear correlations (without controlling for the
 1262 climate modes) between DAOD and ACE, AMM and ENSO indices and ACE are also listed for
 1263 comparison purposes. Correlations that are statistically significant at the 90% level are
 1264 highlighted in bold, and those with asterisks are statistically significant at the 95% level. Note
 1265 that the thresholds for statistical significance are different for partial correlation and linear
 1266 correlation, as the degrees of freedom are different between the two.

	ACE (ctrl. for ENSO)	ACE (ctrl. for AMM)	ACE	ACE (ctrl. for Caribbean DAOD)	ACE (ctrl. for TATL DAOD)
MRC Caribbean DAOD	-0.62*	-0.29	-0.61*	-	-
MRC TATL DAOD	-0.39	-0.07	-0.41	-	-
AMM index (JJA/ASO)	-	-	0.59*/0.45	0.26/0.26	0.48/0.37
ONI (JJA/ASO)	-	-	-0.12/-0.20	0.20/0.18	-0.02/-0.05

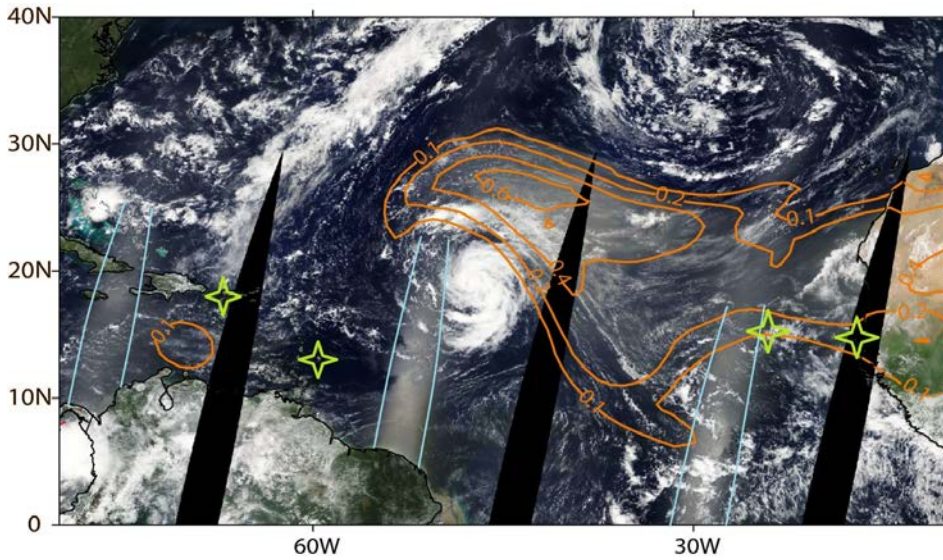
Formatted Table

1267

1268

1269

1270 **Figures:**



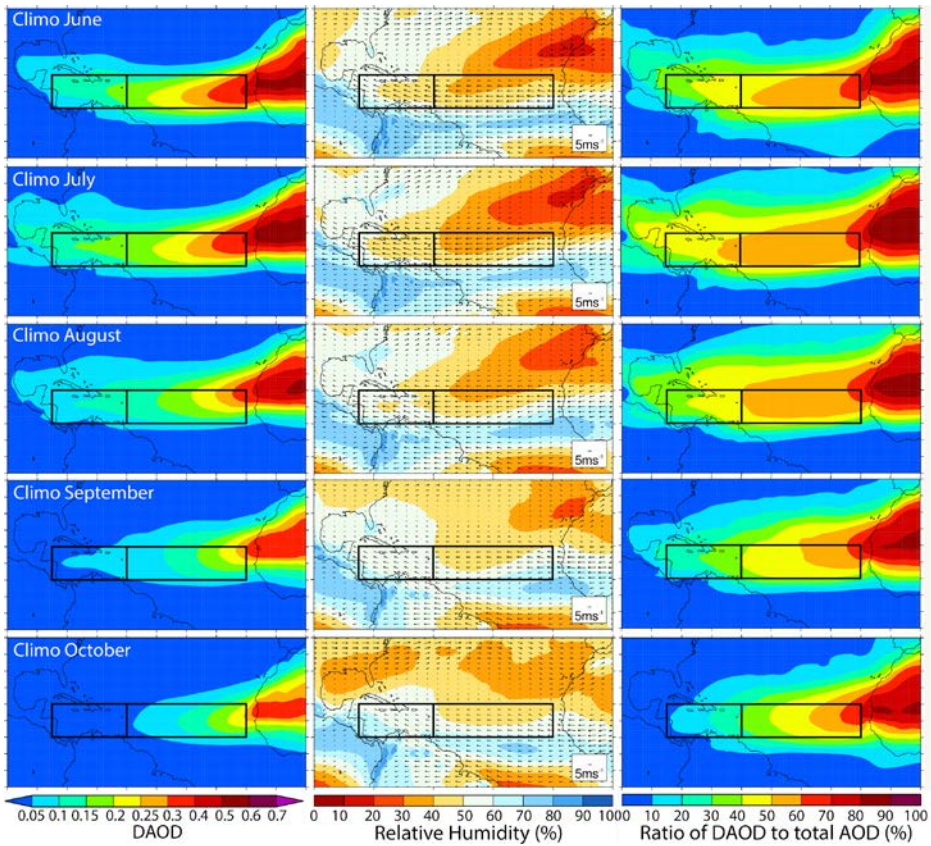
1271

1272 **Figure 1.** True-color Terra MODIS satellite imagery composited on 12 September 2012 and
1273 overlaid with NAAPS-RA 550 nm dust aerosol optical depth (DAOD, an approximate measure
1274 of total atmospheric column of dust aerosol mass, unitless) isopleths, showing Hurricane
1275 Nadine's interaction with the SAL. Nadine is located in the middle of the image. African dust
1276 appears as a light transparent brown haze in between the African coast and Nadine and wrapping
1277 around the northern periphery of the storm. Note that areas of sun glint (narrow regions between
1278 the light blue curves) are similar in color to the dust aerosols, but have the same orientation as
1279 the satellite orbits and are located approximately mid-way between satellite coverage gaps (black
1280 regions oriented south-southwest to north-northeast). Satellite imagery courtesy of the Moderate
1281 Resolution Imaging Spectroradiometer (MODIS) flying on NASA's Terra satellite and available
1282 from <https://worldview.earthdata.nasa.gov/>. The stars in light green represent four sites used for
1283 validation purposes, including Dakar, Capo Verde, Ragged Point and La Parguera in order from
1284 east to west.

1285

1286

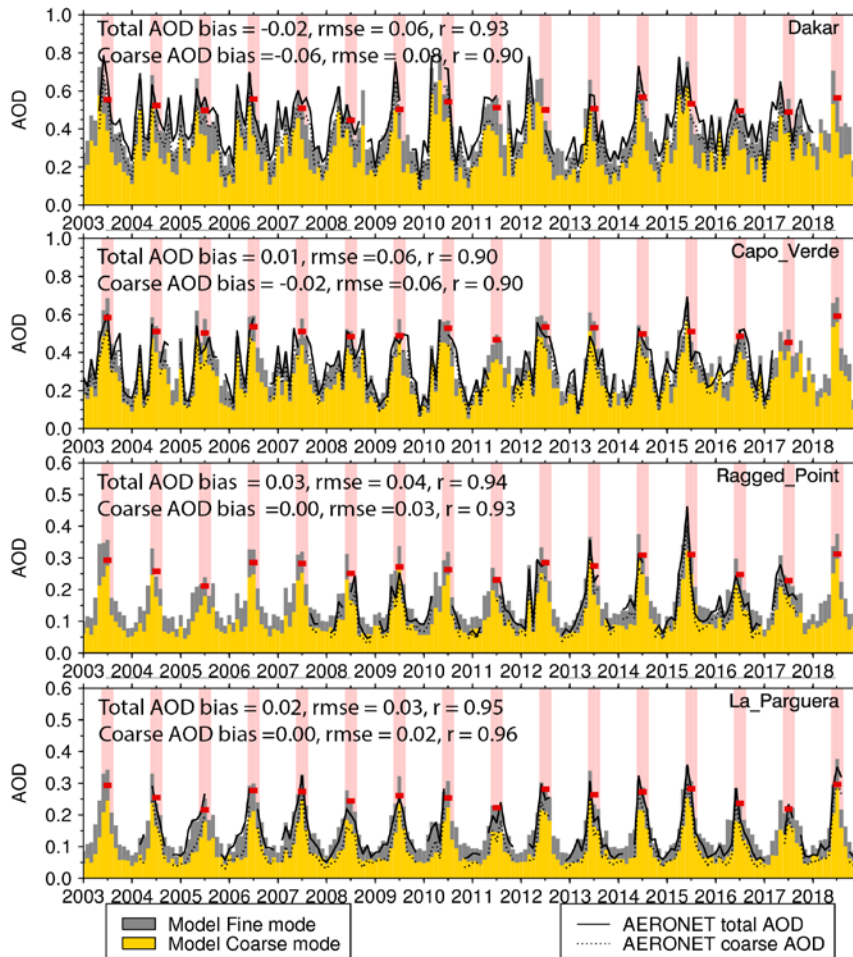
1287



1288

1289 **Figure 2.** Climatological (2003-2018 average) monthly mean DAOD (left column) and the ratio
1290 of DAOD to total AOD (right column) for June-October based on the MRC. The middle column
1291 shows the climatological 700 hPa RH (color shading) and horizontal wind vectors from ERA-
1292 Interim. Black boxes denote the MDR, including the Caribbean (left, 10°-20°N, 85°-60°W) and
1293 the tropical North Atlantic (right, 10°-20°N, 60°-20°W, denoted “TATL”).

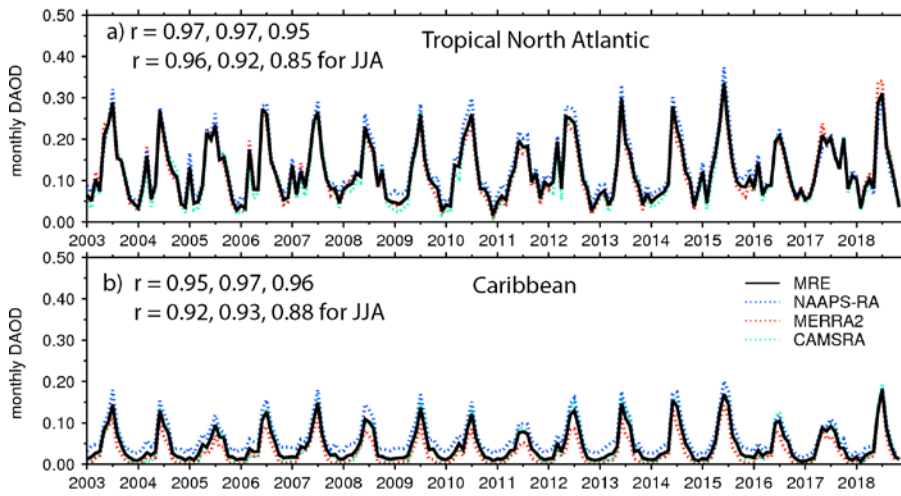
1294



1295

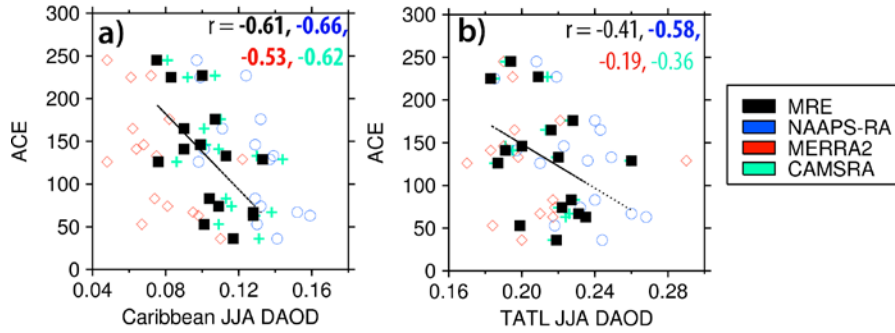
1296 **Figure 3.** Monthly mean Version 3 L2 AERONET and MRC 550nm modal AODs at four
 1297 African dust-impacted sites: Dakar, Cape Verde, Ragged Point and La Parguera from east to
 1298 west. JJA are highlighted with pink shading, and JJA seasonal average total AOD from MRC are
 1299 shown with red bars. Annotations for each time series show bias, RMSE and correlation (r) of
 1300 monthly averages calculated from the MRC.

1301



1303 **Figure 4.** Monthly DAOD at 550nm from CAMSRA, MERRA-2, NAAPS-RA and MRC from
 1304 2003-2018 for the (a) tropical North Atlantic and the (b) Caribbean. Correlations between
 1305 CAMSRA and MERRA-2, CAMSRA and NAAPS-RA, MERRA-2 and NAAPS-RA are
 1306 displayed in sequence for all months and for JJA-only respectively.
 1307

1308

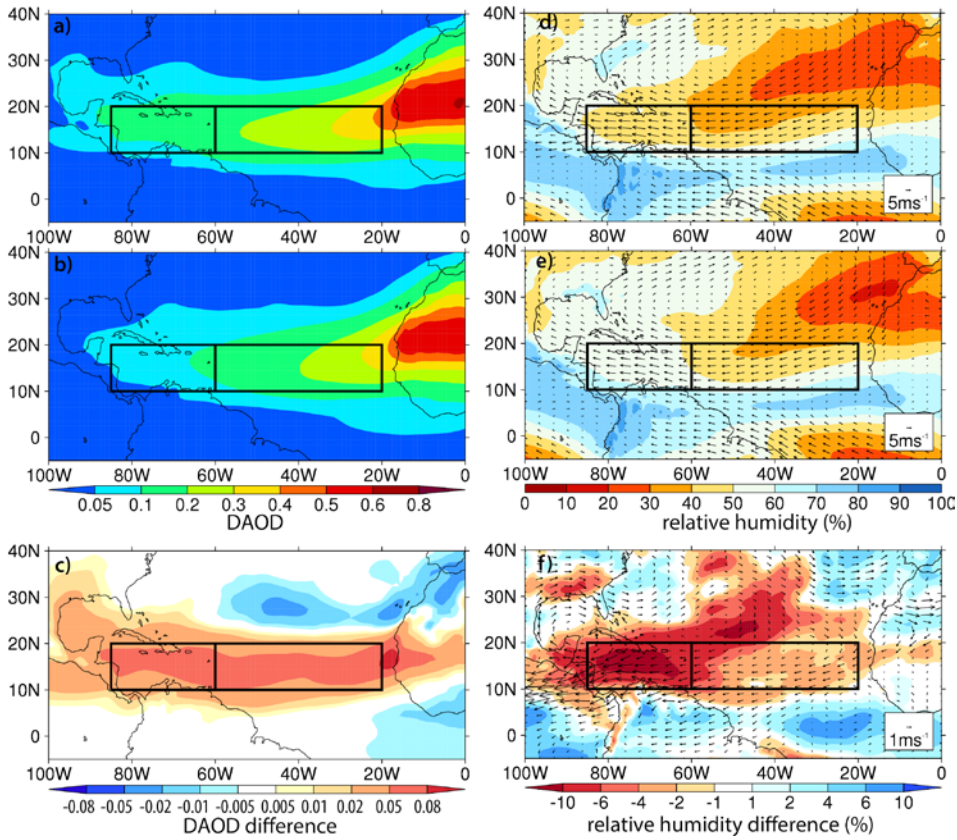


1309

1310 **Figure 5.** Scatterplot showing the relationship between annual Atlantic Accumulated Cyclone
1311 Energy (ACE) and JJA region-averaged DAOD from MRC, NAAPS-RA, MERRA-2 and
1312 CAMSRA over the (a) Caribbean and (b) the tropical North Atlantic. One unit of ACE equals 10^4
1313 kt^2 . Correlations (r) between ACE and DAOD are color-coded for different DAOD products and
1314 overlaid on each plot, and statistically significant correlations are in bold. The possible causes of
1315 the DAOD difference between the reanalysis products are discussed in Section 3.1.

1316

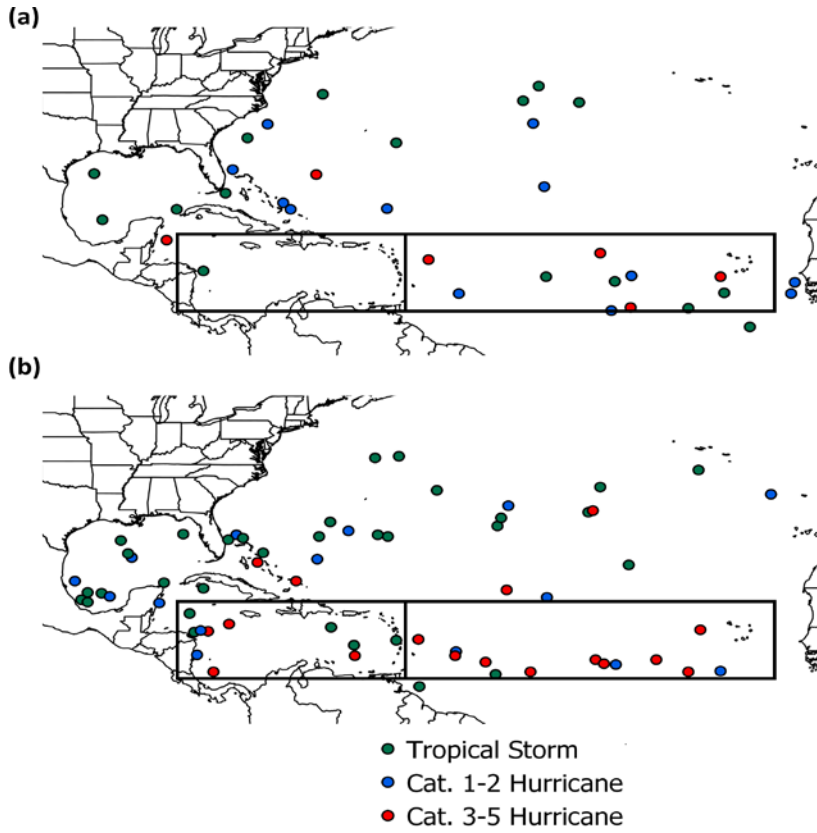
1317



1318 **Figure 6.** Left: MRC JJA composite of DAOD for the three Atlantic hurricane seasons from
1319 2003-2018 with (a) the highest JJA Caribbean DAOD (2014, 2015 and 2018), (b) the lowest JJA
1320 Caribbean DAOD (2005, 2011, and 2017), and (c) the difference between the two (highest minus
1321 lowest). Right: The corresponding JJA composite of 850 hPa wind (vectors) and 700 hPa RH
1322 (color shading).
1323

1324

1325

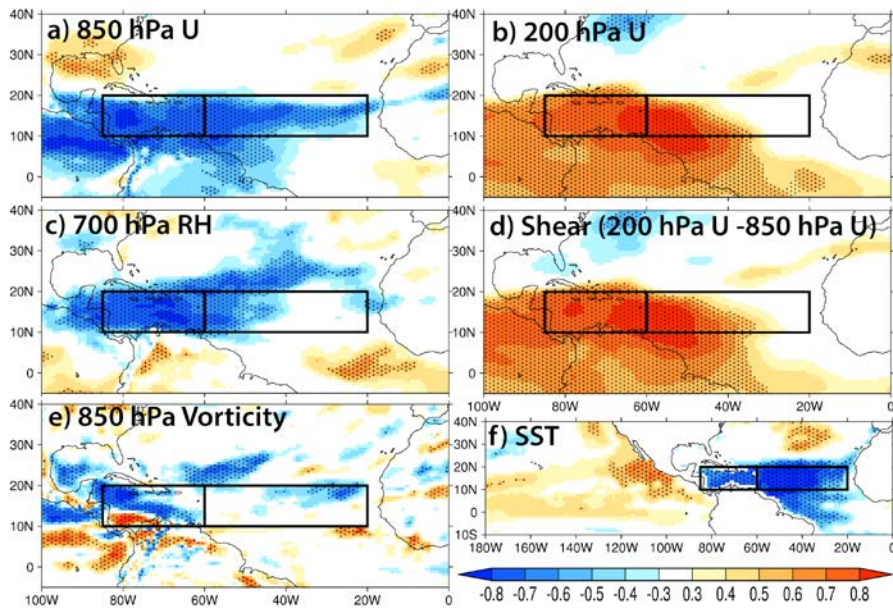


1326

1327

1328 **Figure 7.** Formation locations of Atlantic named storms during the three seasons with (a) the
1329 highest Caribbean JJA DAOD (2014, 2015 and 2018) and (b) the lowest Caribbean JJA DAOD
1330 (2005, 2011, and 2017). Also displayed are the maximum intensity that each TC reached.

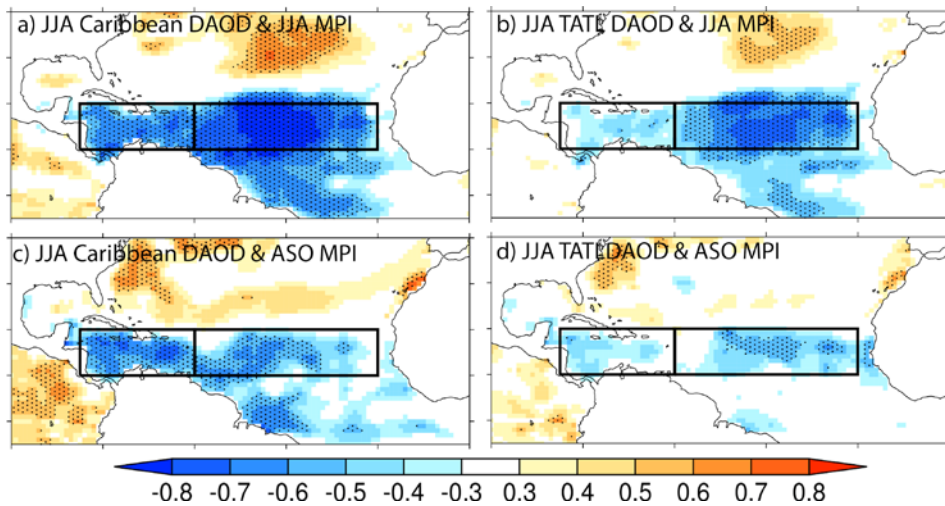
1331



1332
 1333 **Figure 8.** Correlation between MRC JJA regionally-averaged DAOD in the Caribbean and JJA
 1334 (a) 850 hPa U, (b) 200 hPa U, (c) 700 hPa RH, (d) zonal wind shear, (e) 850 hPa relative
 1335 vorticity and (f) SST. Correlations over the black dotted areas are statistically significant.

1336

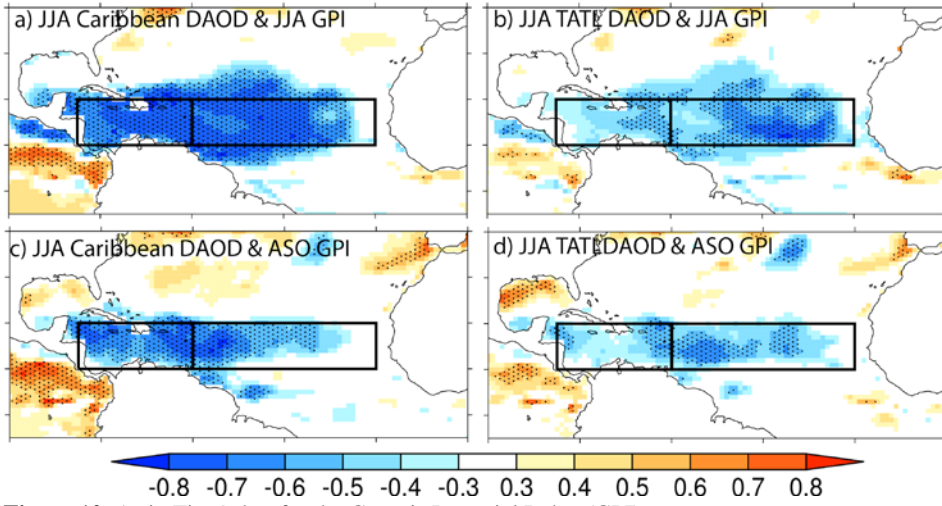
1337



1338

1339 **Figure 9.** Correlation between (a) MRC JJA regionally-averaged DAOD in the Caribbean and
 1340 JJA Maximum Potential Intensity (MPI), (b) MRC JJA regionally-averaged DAOD in the
 1341 tropical North Atlantic (TATL) and JJA MPI, (c) JJA Caribbean DAOD and ASO MPI and (d)
 1342 JJA TATL DAOD and ASO MPI. Correlations over the black dotted areas are statistically
 1343 significant.

1344



1345

1346

Figure 10. As in Fig. 9, but for the Genesis Potential Index (GPI).

1347

1348